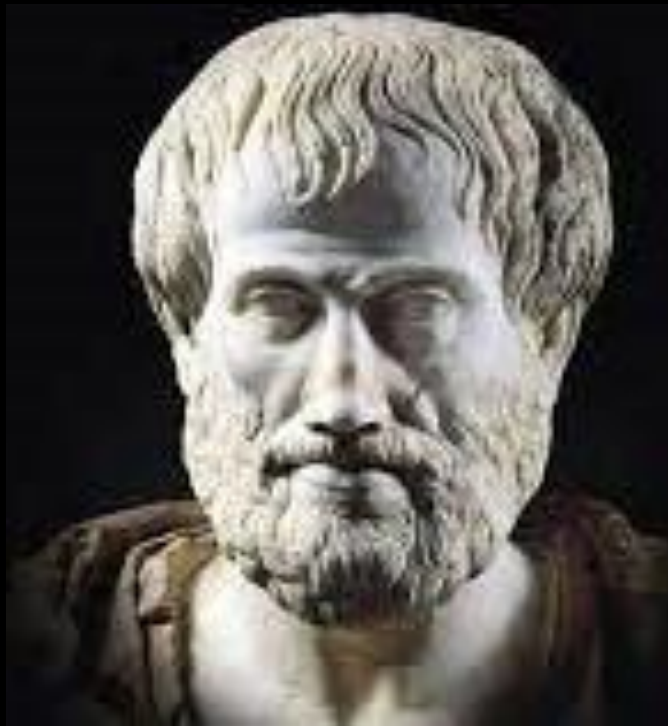
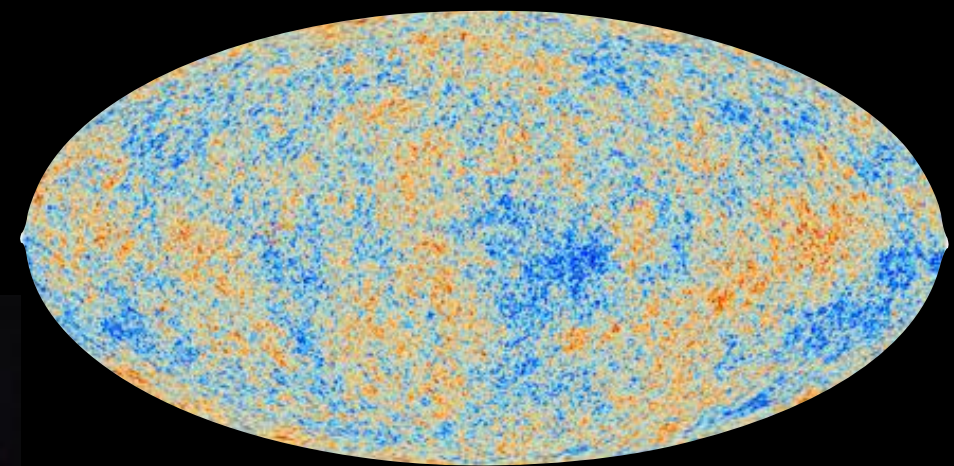
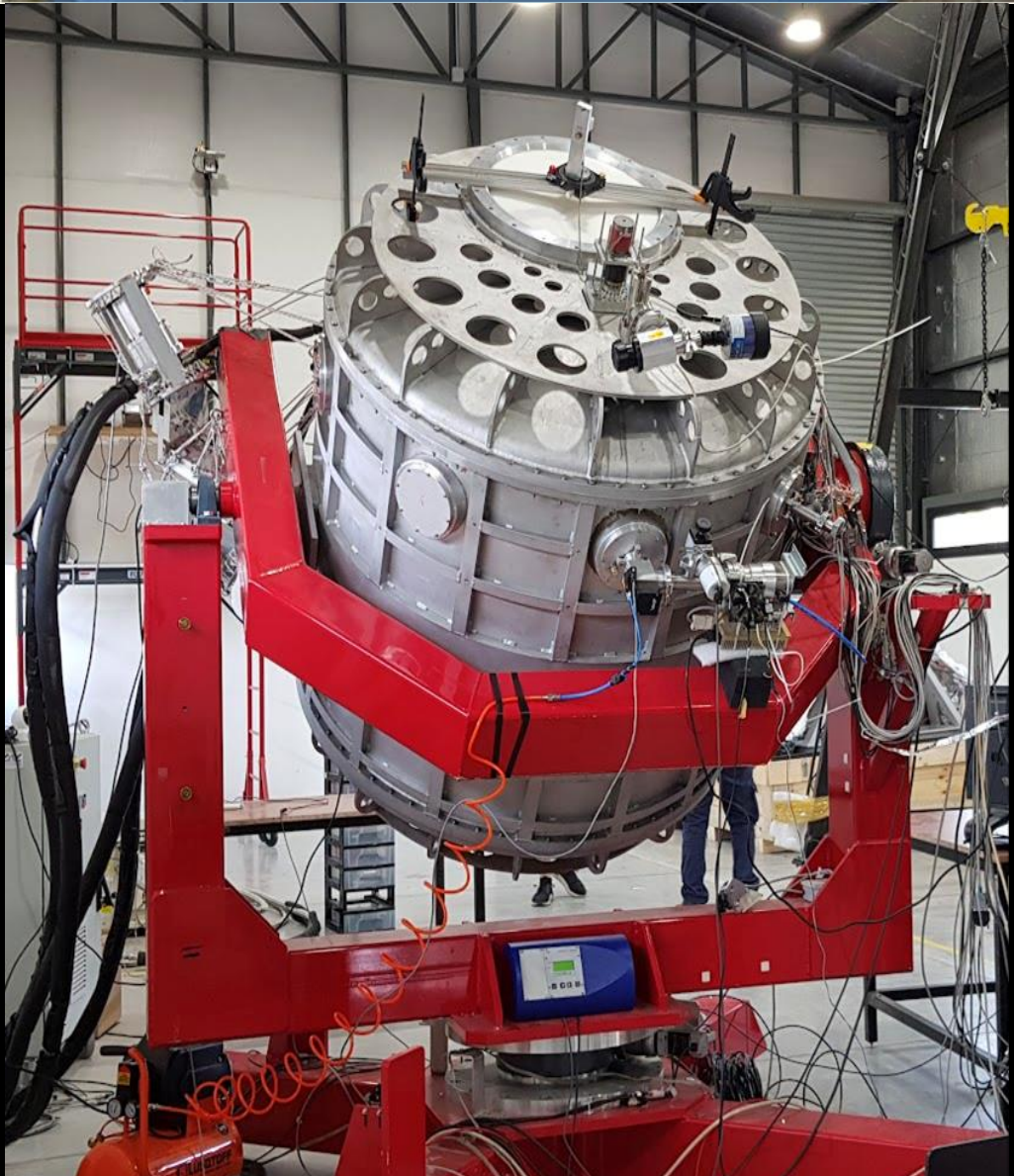




CMB measurements with mm- telescopes



*S. Loucatos
Irfu CEA-Saclay and
APC Paris
HEP Thessaloniki
2022*

**no published errata*

$z < 2 \times 10^6$
Thermal history
(energy injection into the CMB)

CMB T,E (B)
Cosmological model

CIB, cosmological
astrophysics

Inflation

Quantum
Fluctuations

ISM

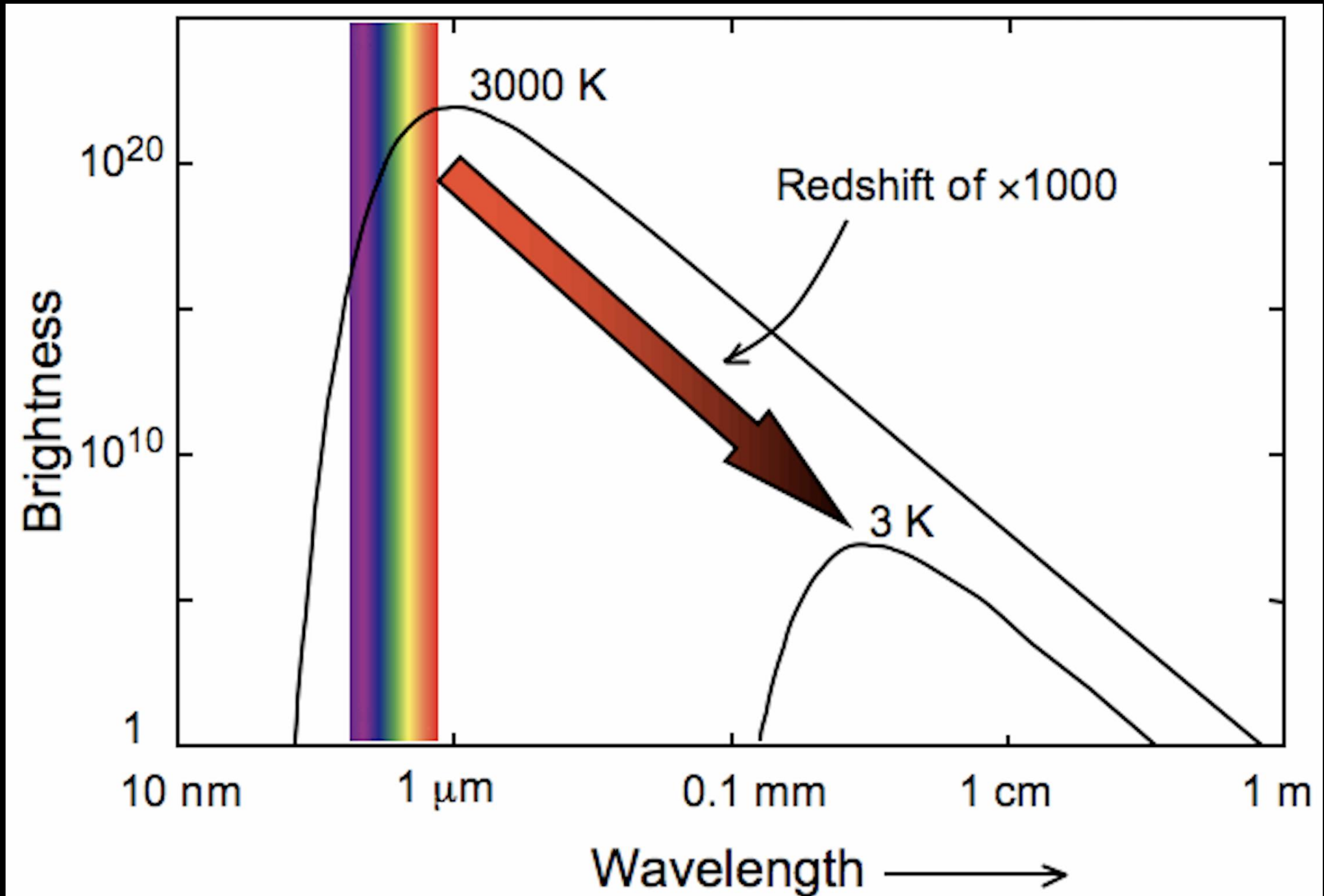
$z \approx 6-11$
Reionization

Inflation
Physics at $\approx 10^{16}$ GeV
 $E > 10^{12} \times E_{\text{LHC}}$

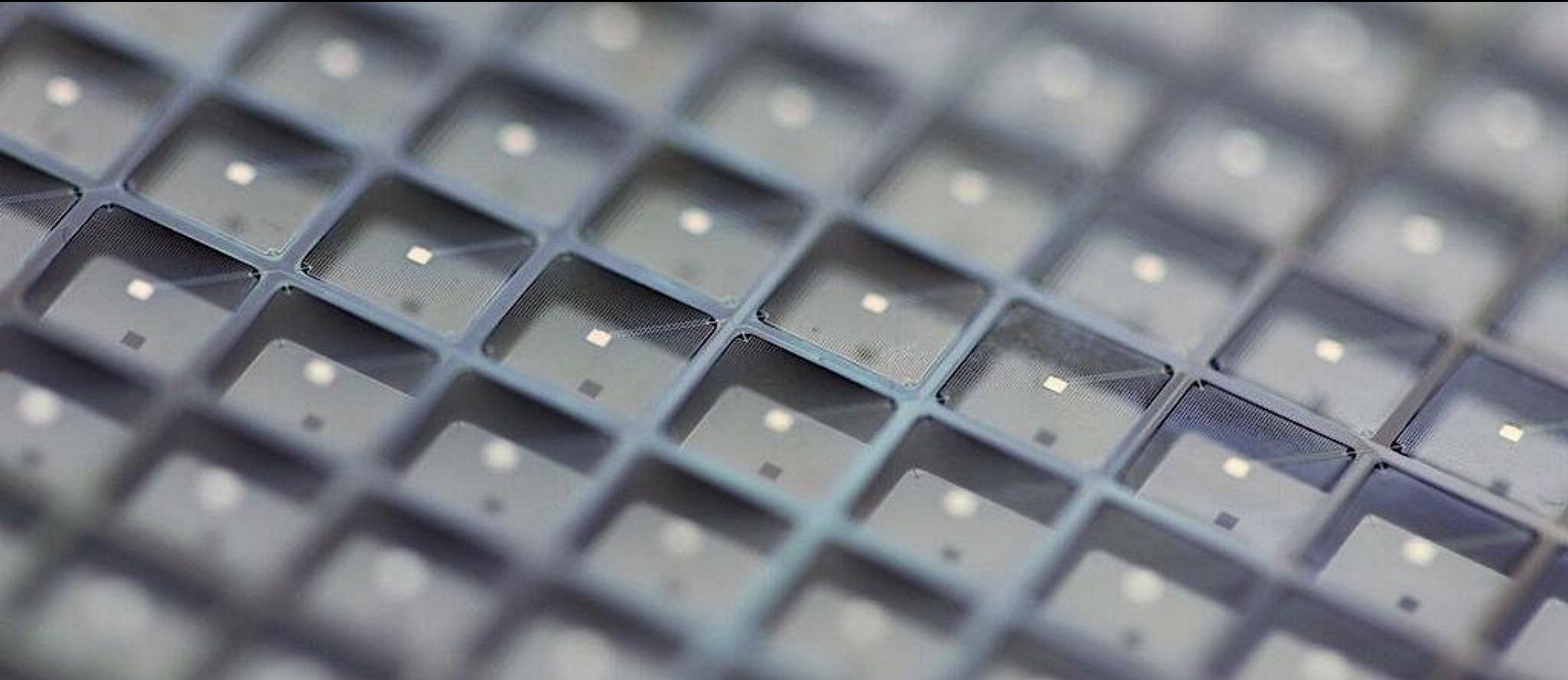
$z \approx 1-3$
Gravitational lensing
Dark matter distribution

$z \approx 0-2$
Sunyaev-Zeldovich effect:
Distribution of the hot gas
and velocity field

Radiation emitted at 3000K → cooled by universe expansion to 2.77 K

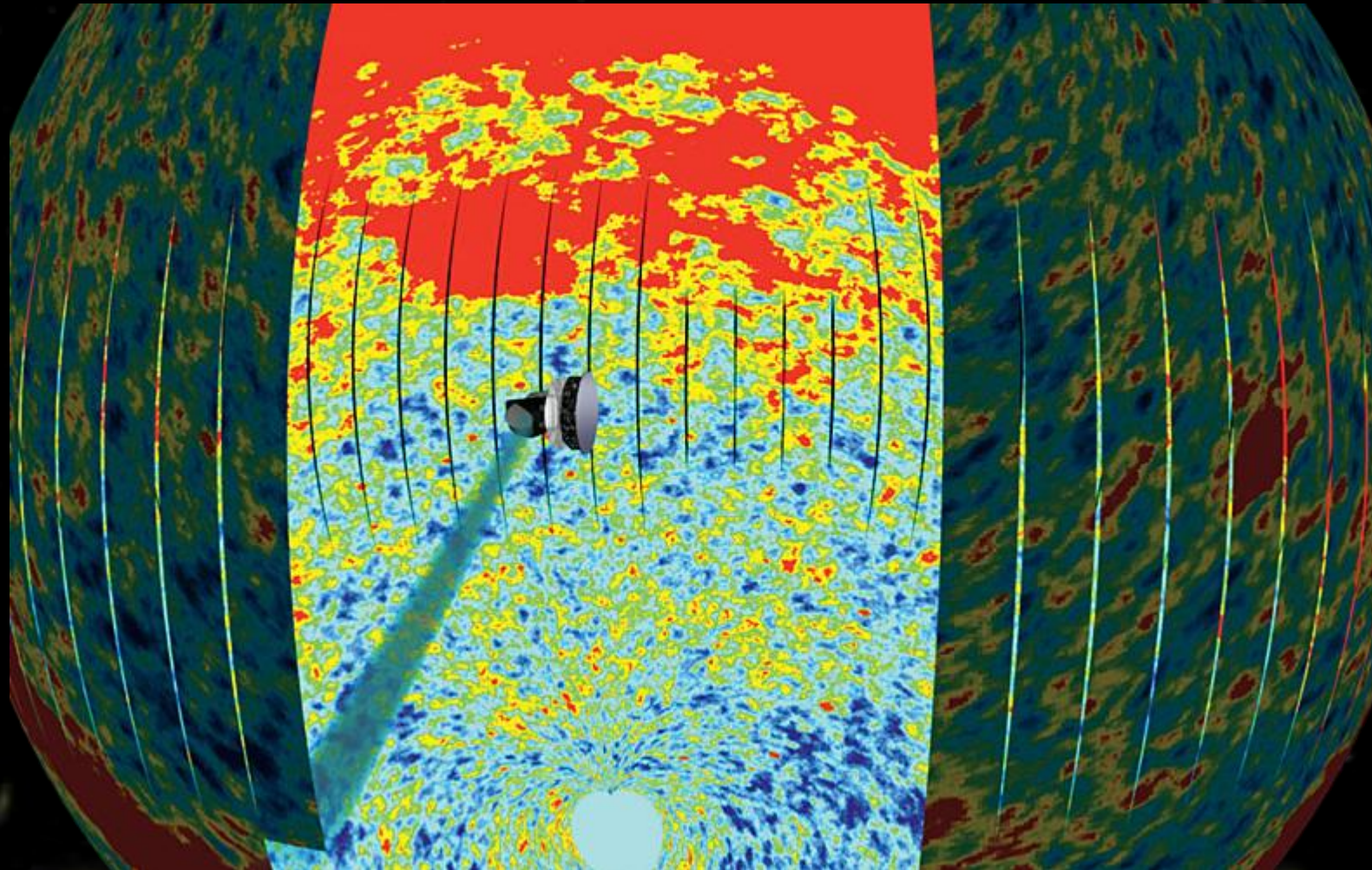


Environment of the detectors $< T_{\text{CMB}}$
Thermometers (bolometers) cooled at 100 -300 mK
→ minimize the thermal noise (phonons)





Many pixels = imager



Planck sky scan



The CMB as a window to study cosmic inflation

Radius of the Visible Universe

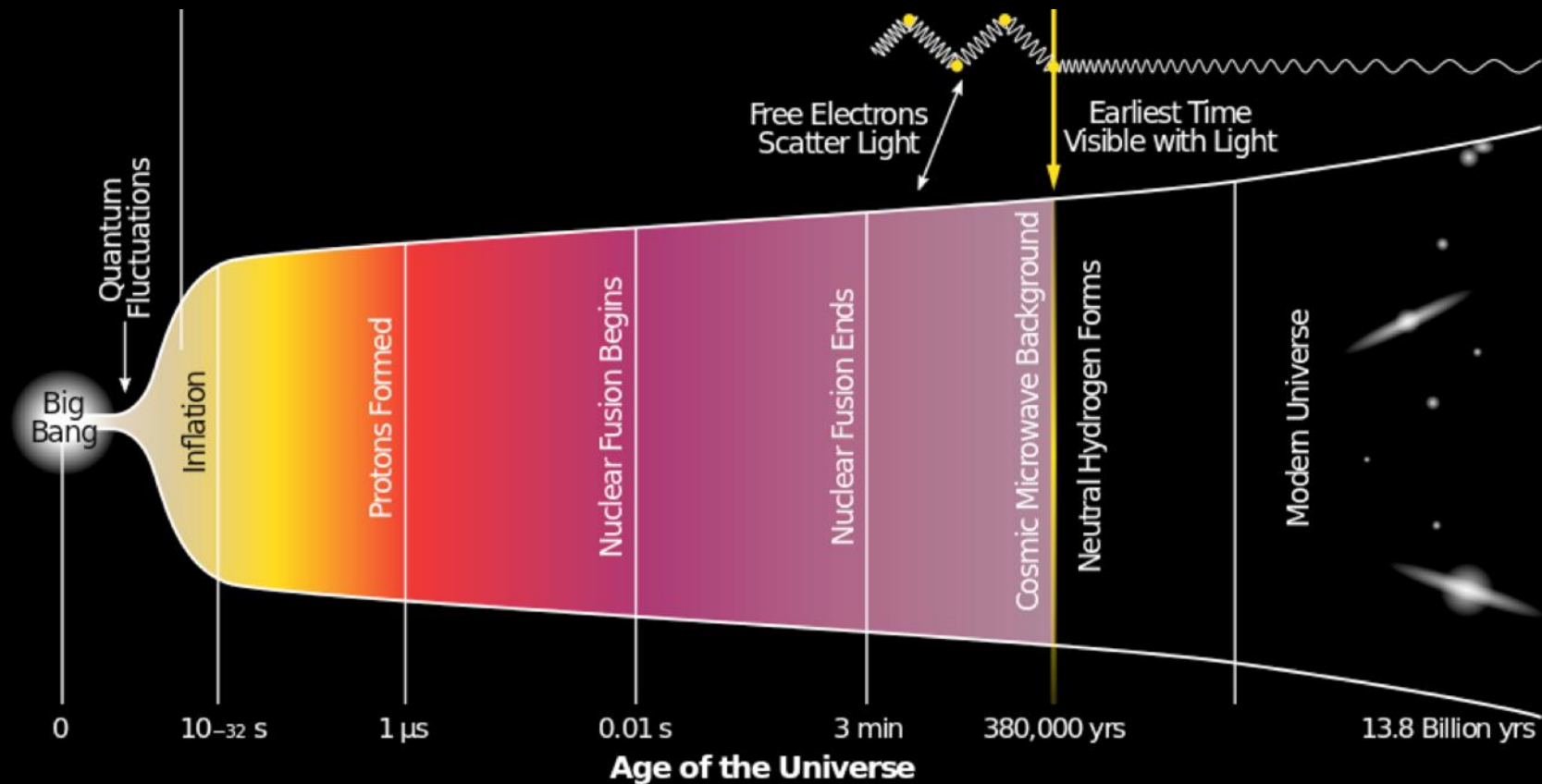
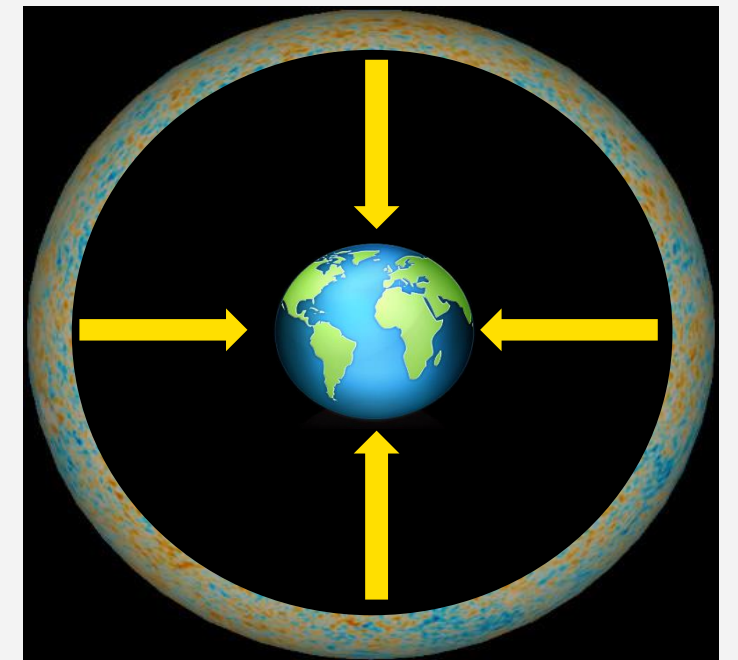
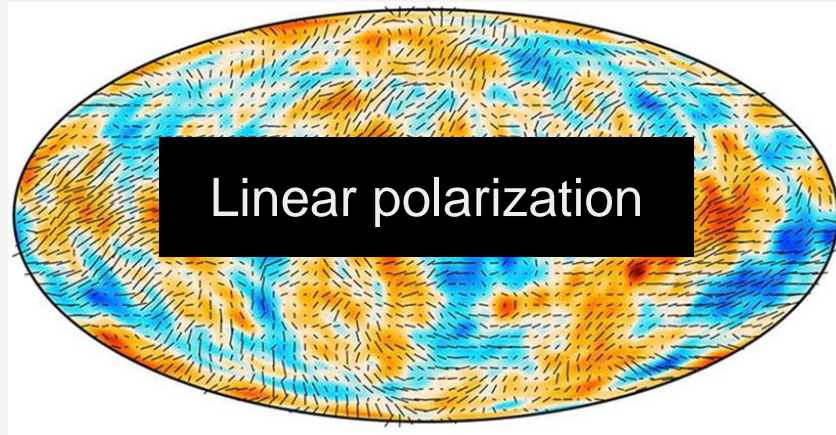


Image : BICEP/Keck



L. Mousset Blois 2022

The CMB as a window to study cosmic inflation



E
modes



B modes

Radius of the Visible Universe

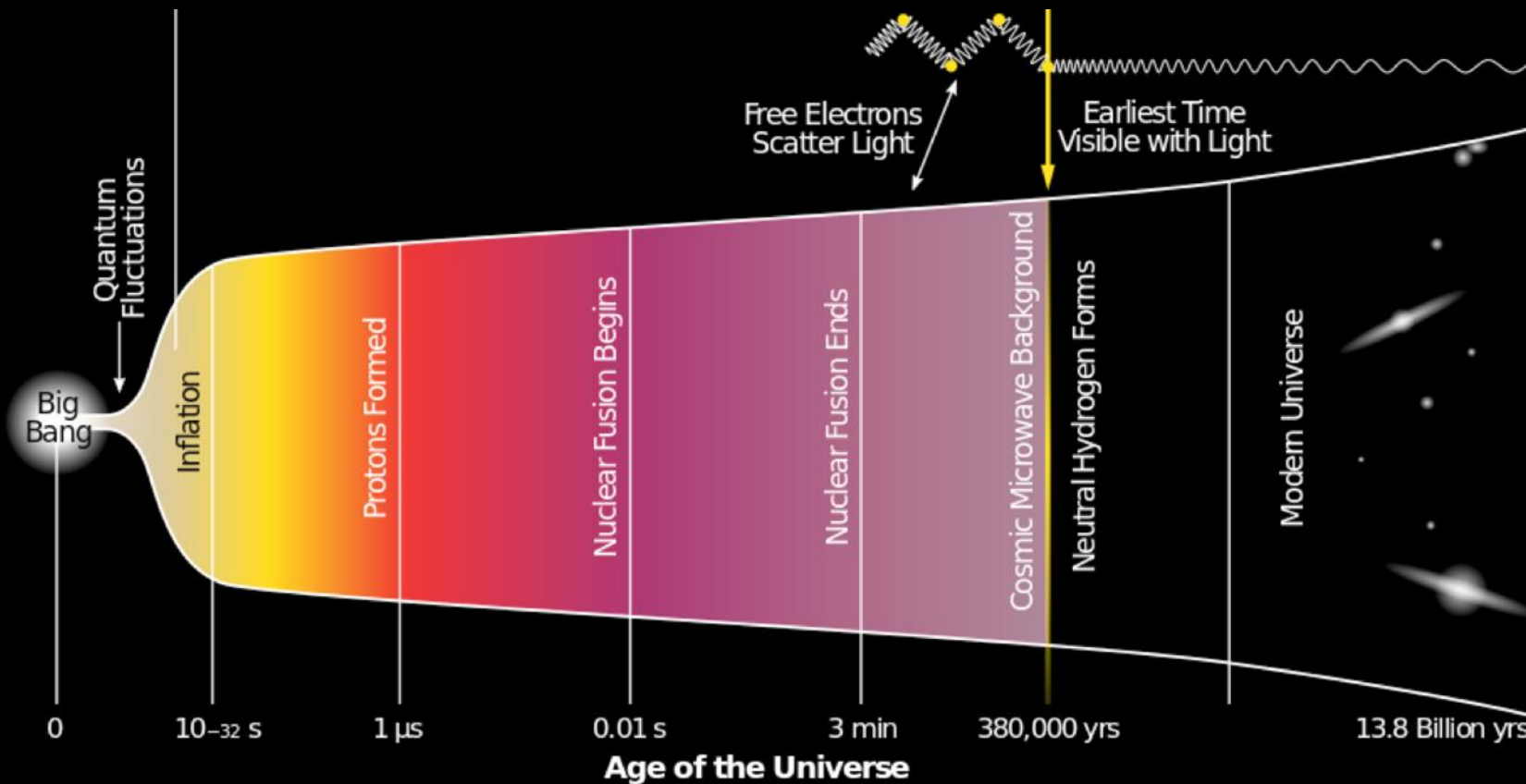


Image : BICEP/Keck



The CMB as a window to study cosmic inflation

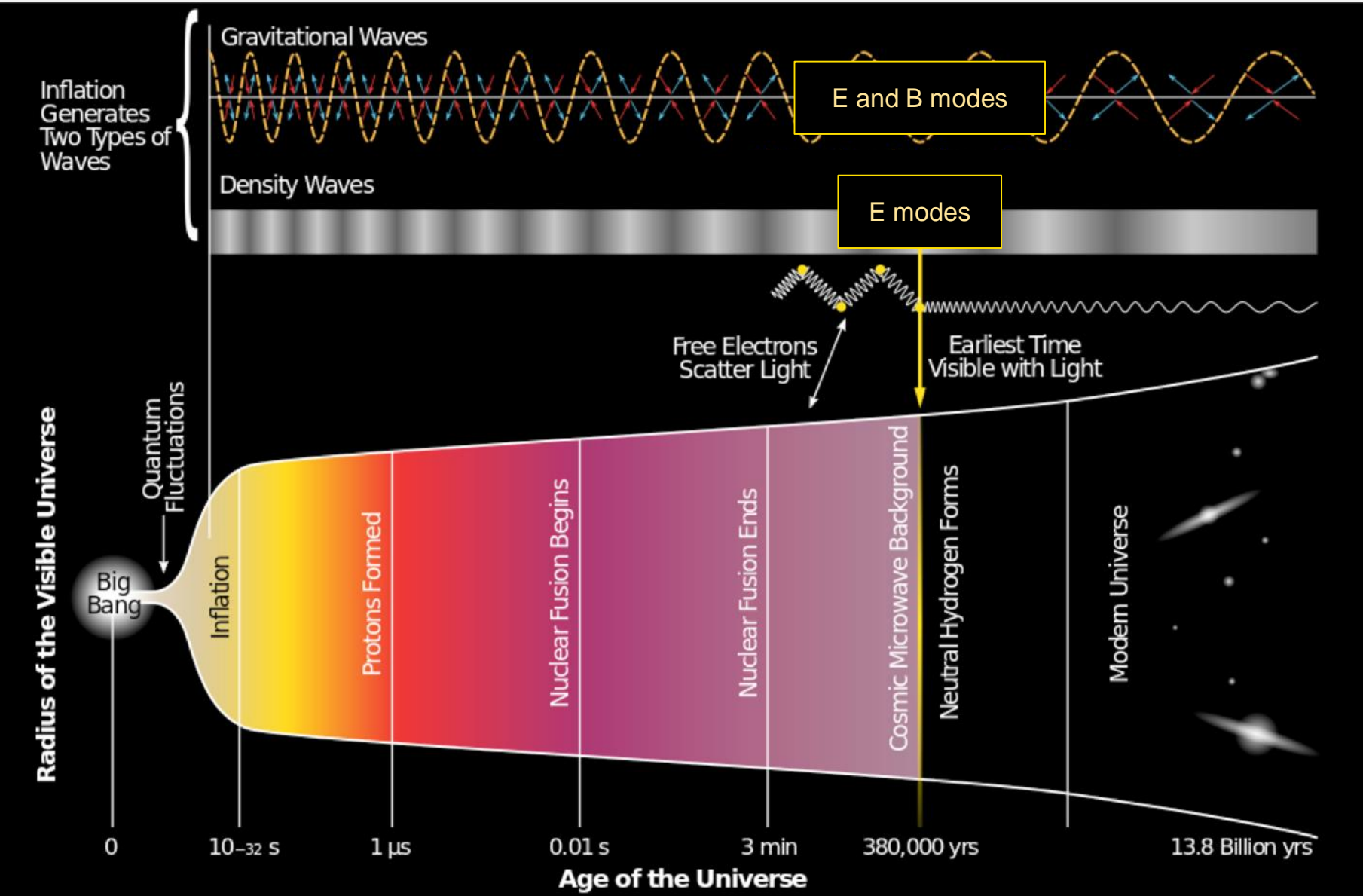
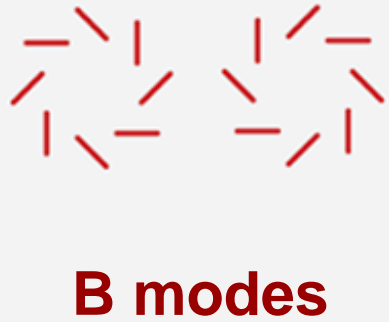
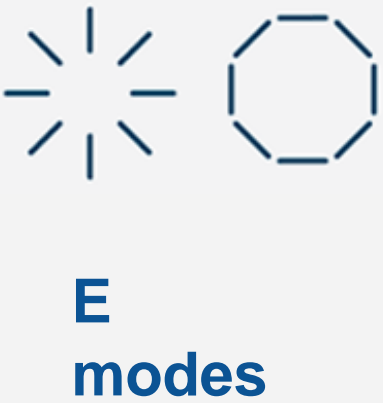
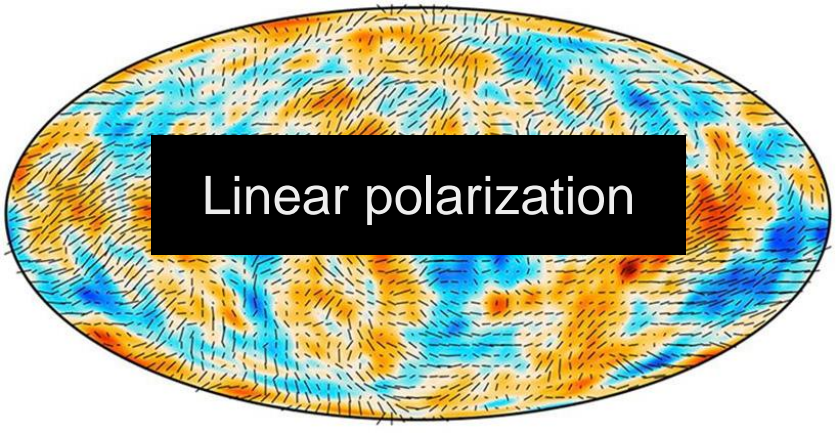
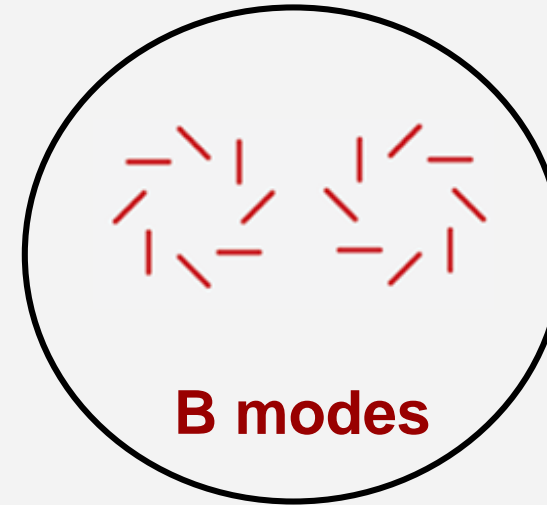
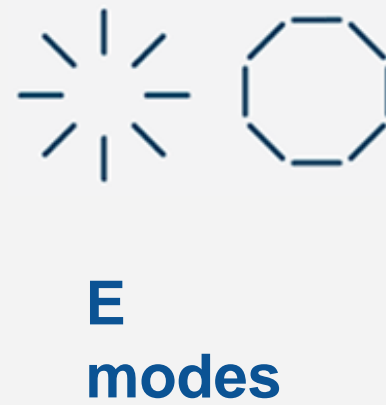
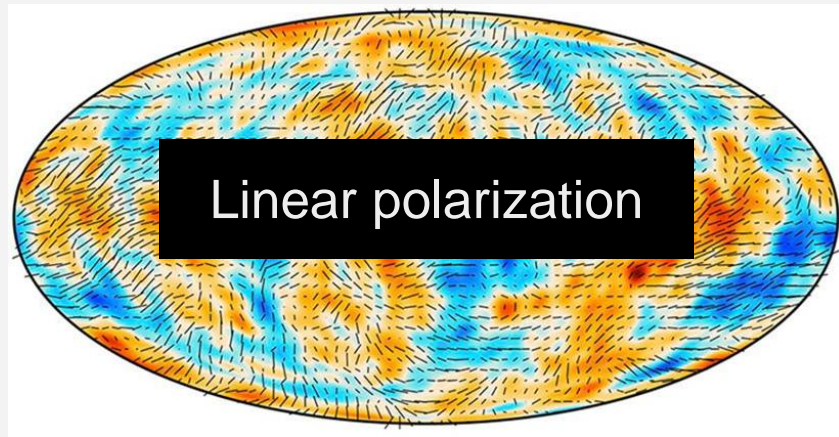


Image : BICEP/Keck

The CMB as a window to study cosmic inflation

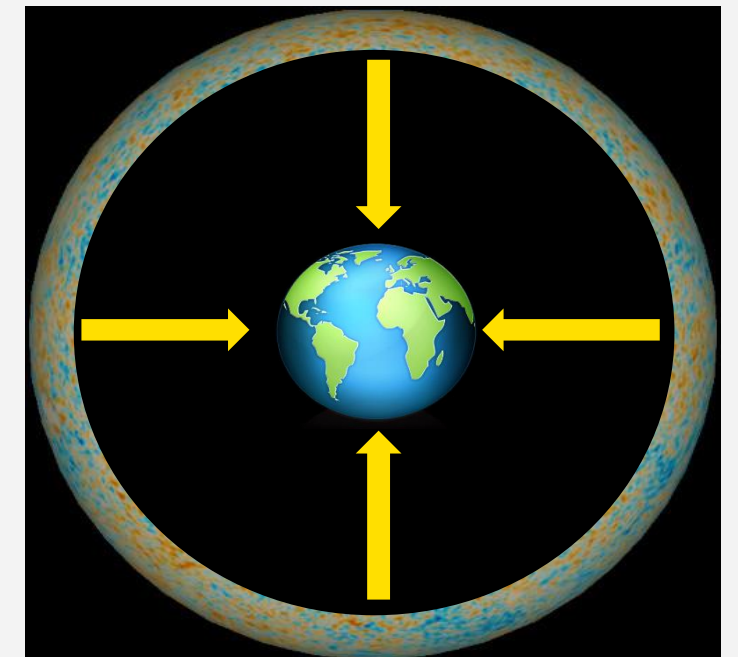
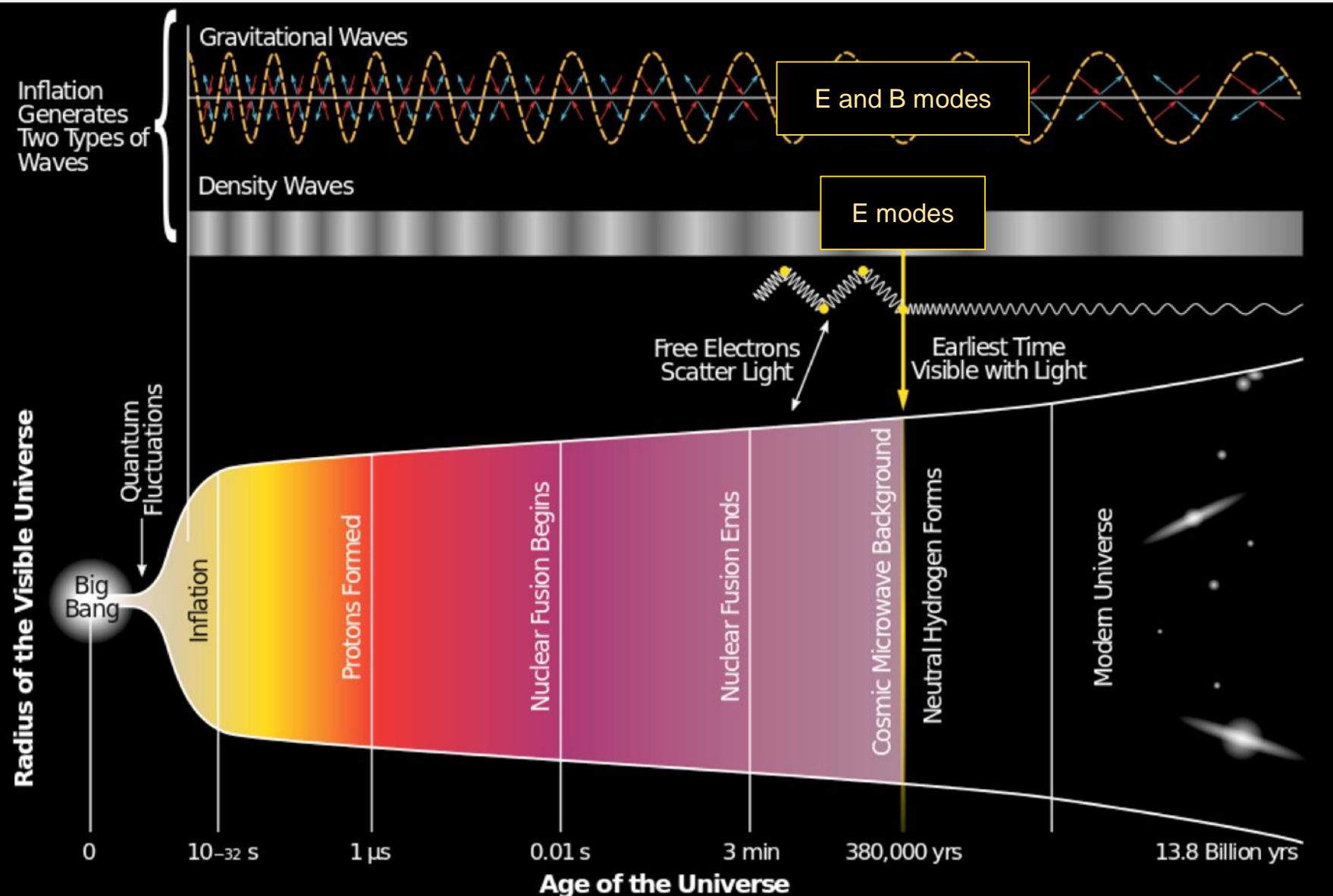


The amplitude is parametrized by the tensor to scalar ratio r .

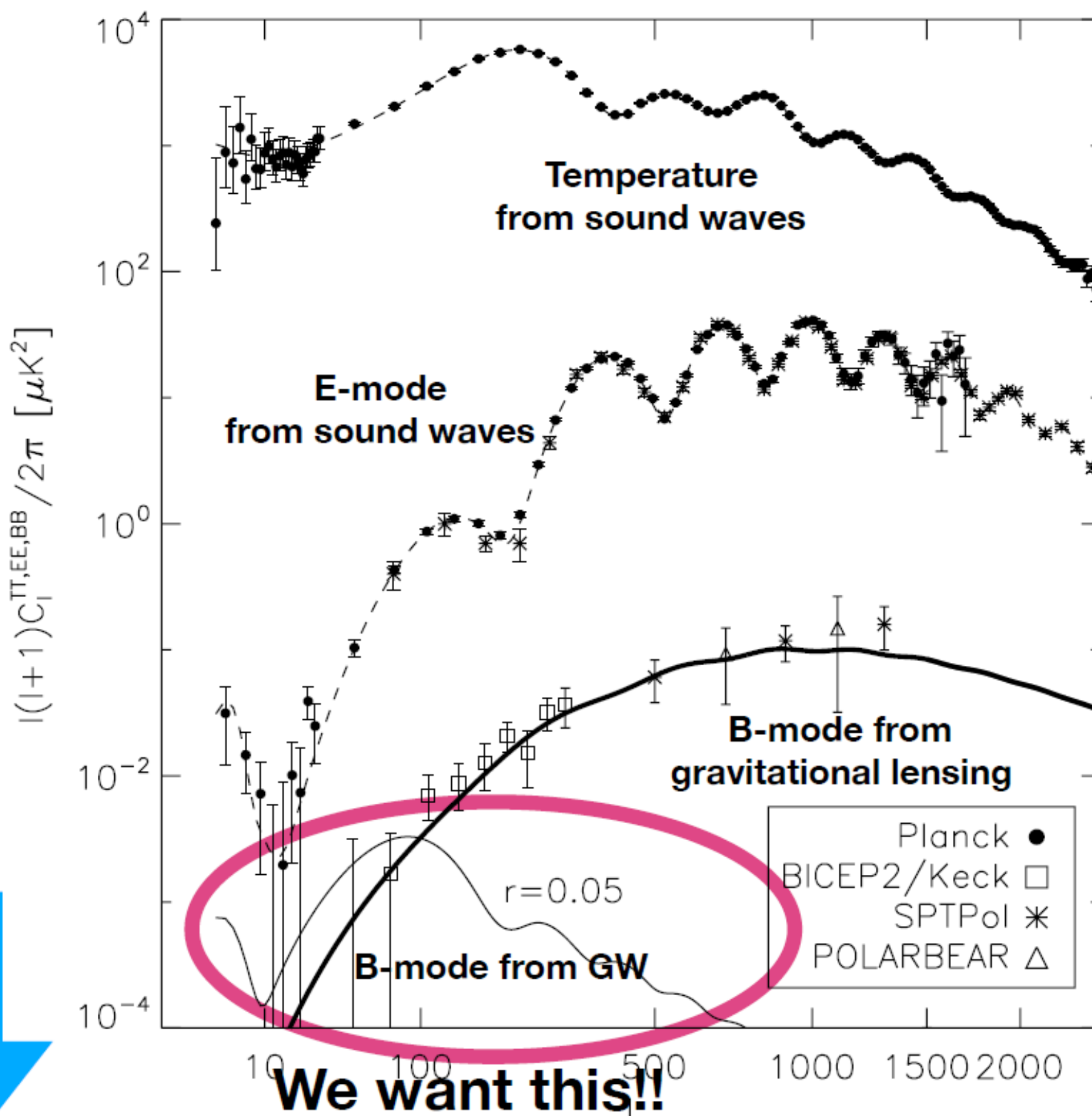
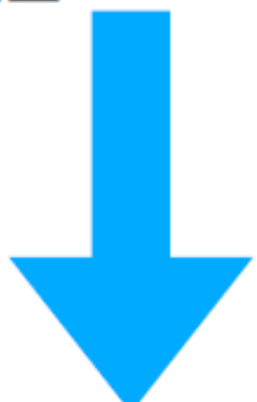
Current upper limit:

$$r < 0.032 \text{ à } 95\% \text{ C.L.}$$

[Tristram et al., 2022, BICEP/Keck]



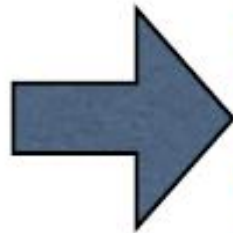
Another two orders of magnitude
in the next 10–15 years



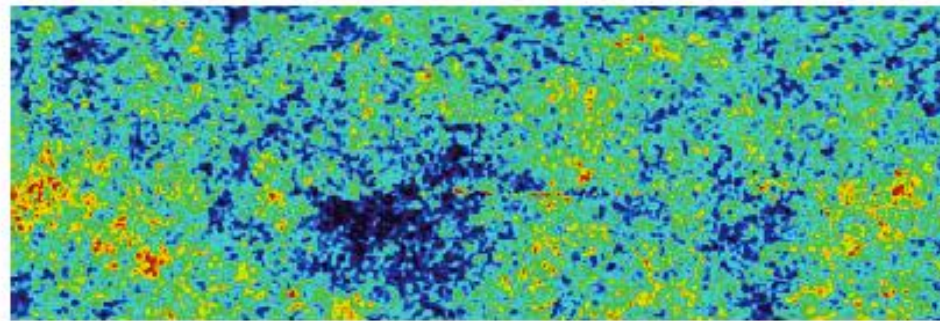
Key Predictions

ζ

scalar
mode



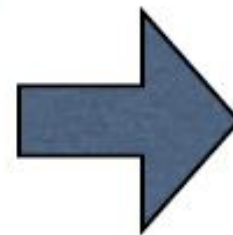
- Fluctuations we observe today in CMB and the matter distribution originate from quantum fluctuations during inflation



Mukhanov&Chibisov (1981)
Guth & Pi (1982)
Hawking (1982)
Starobinsky (1982)
Bardeen, Steinhardt&Turner (1983)

h_{ij}

tensor
mode



- There should also be *ultra long-wavelength* gravitational waves generated during inflation



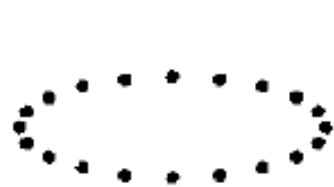
Grishchuk (1974)
Starobinsky (1979)

We measure distortions in space

- A distance between two points in space

$$d\ell^2 = a^2(t)[1 + 2\zeta(\mathbf{x}, t)][\delta_{ij} + h_{ij}(\mathbf{x}, t)]dx^i dx^j$$

- ζ : “curvature perturbation” (scalar mode)
 - Perturbation to the determinant of the spatial metric
- h_{ij} : “gravitational waves” (tensor mode)
 - Perturbation that does not alter the determinant

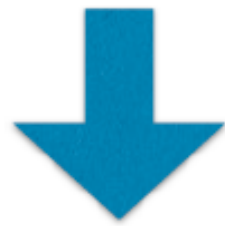


$$\sum_i h_{ii} = 0$$

Measuring GW

- GW changes distances between two points

$$d\ell^2 = d\mathbf{x}^2 = \sum_{ij} \delta_{ij} dx^i dx^j$$



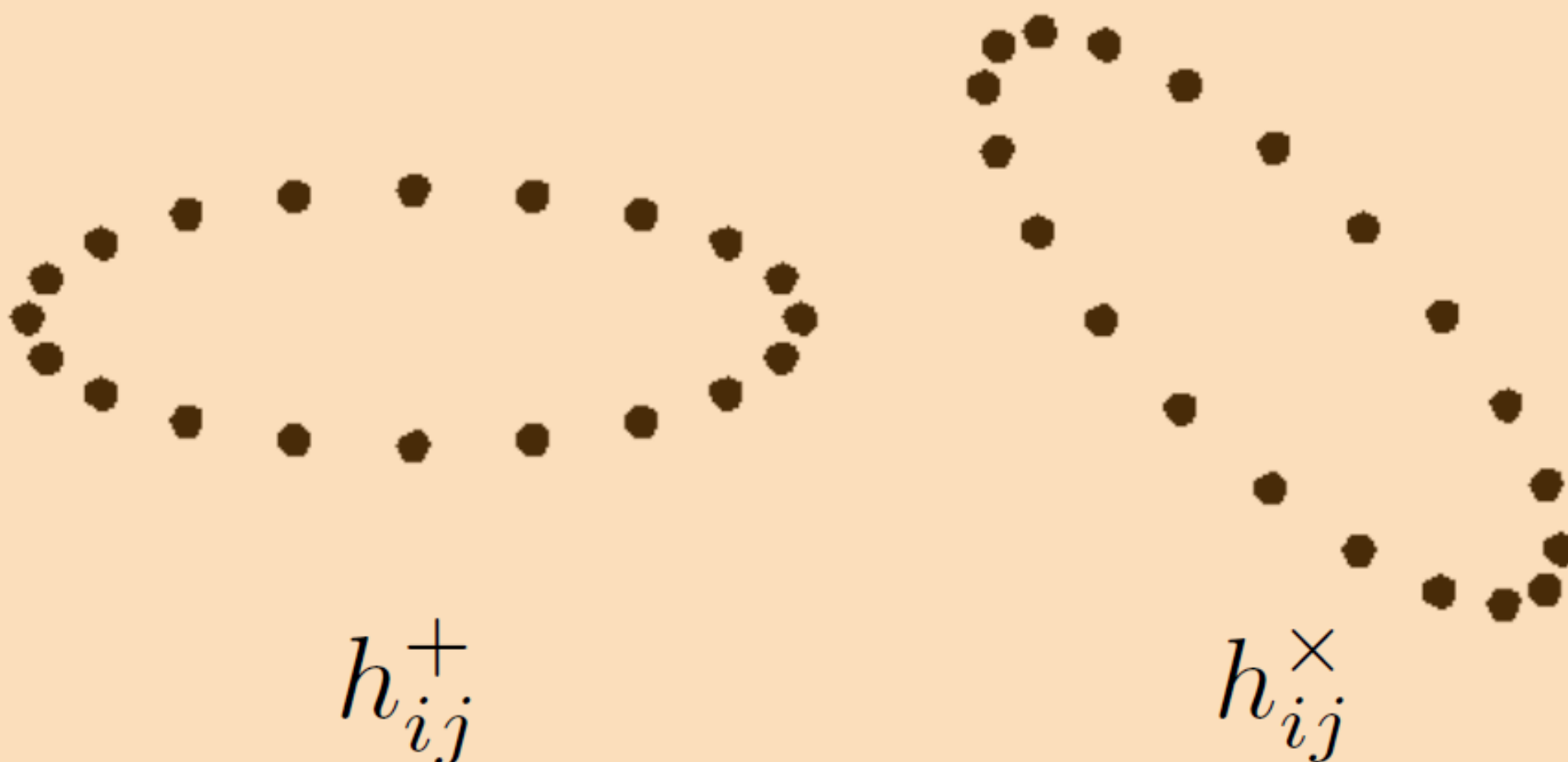
$$d\ell^2 = \sum_{ij} (\delta_{ij} + \underline{h_{ij}}) dx^i dx^j$$



Laser interferometers LIGO and VIRGO detected GW from binary Blackholes and NS, with the wavelength of thousands of kilometres
But, the primordial GW affecting the CMB has a wavelength of **billions of light-years!!** How do we find it?

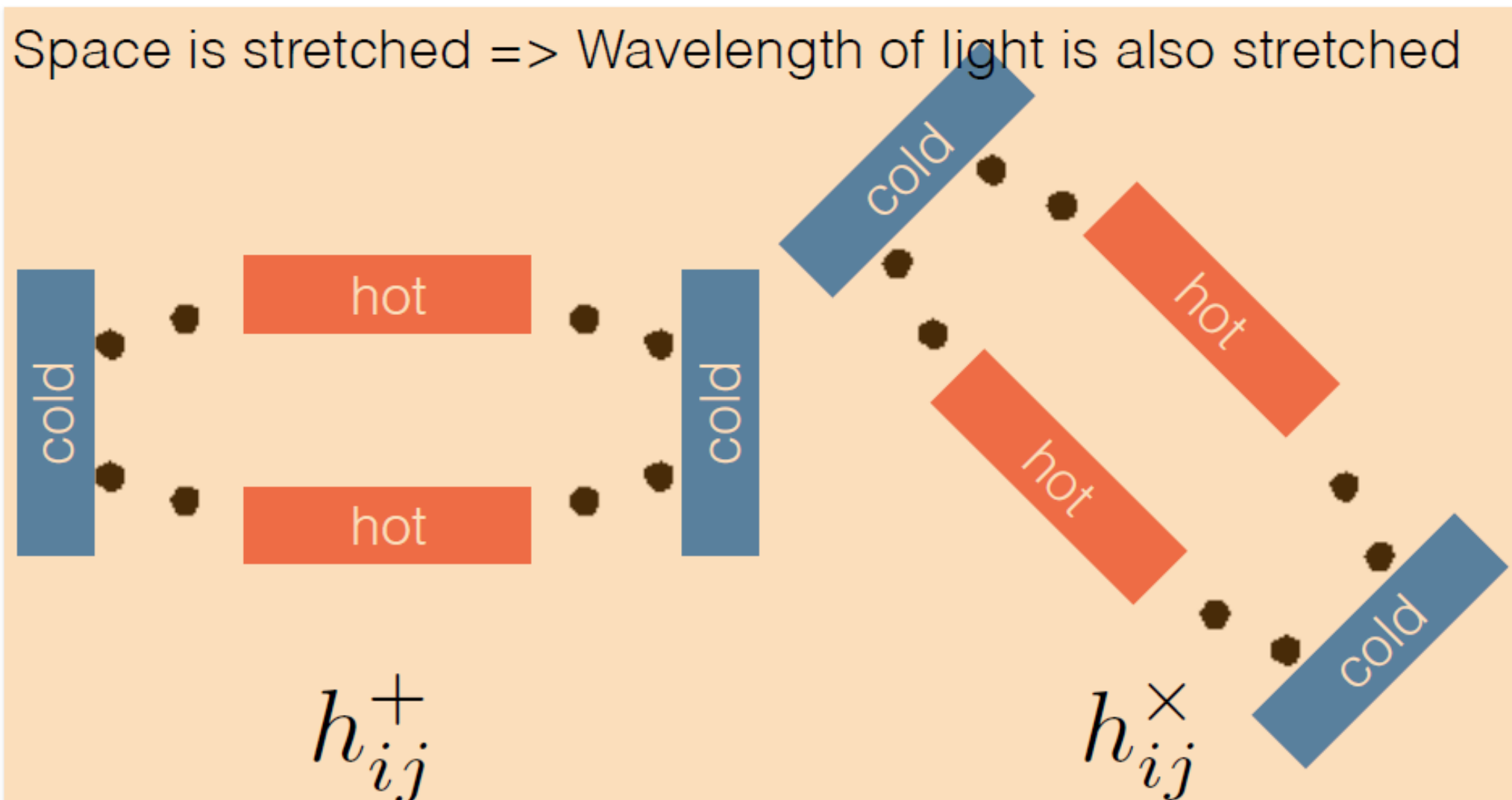
Detecting GW by CMB

GW propagating in isotropic electro-magnetic fields

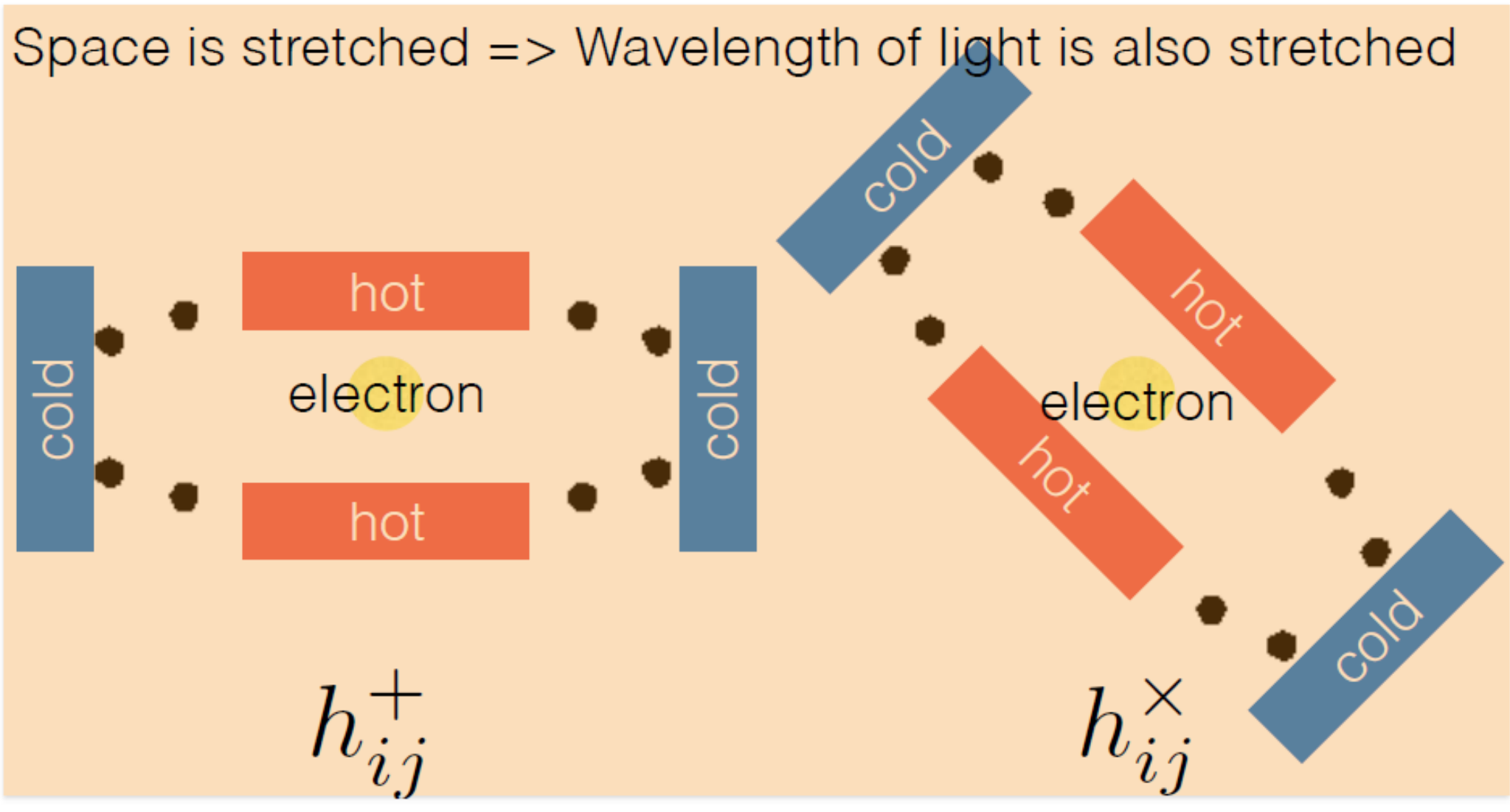


Detecting GW by CMB

Space is stretched => Wavelength of light is also stretched

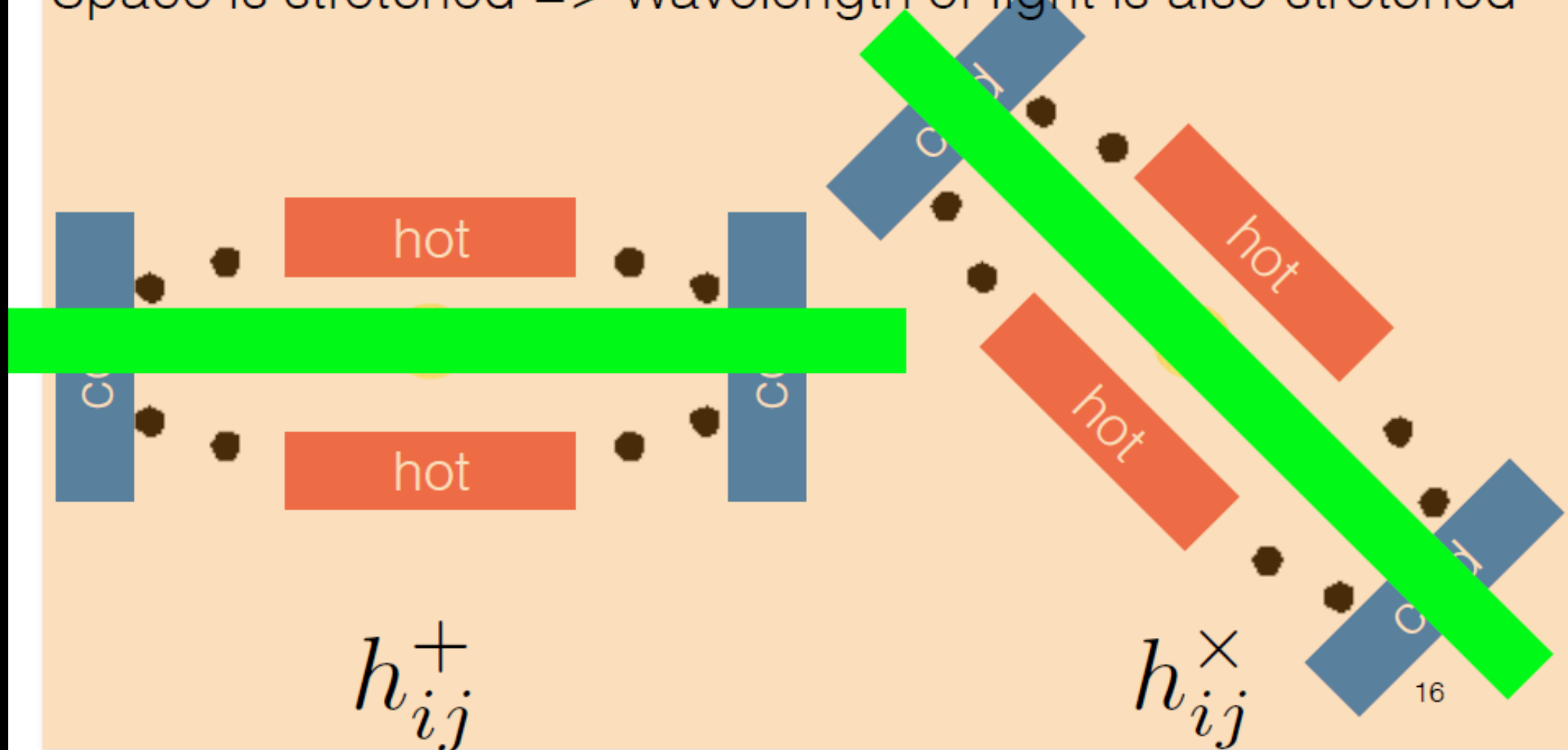


Detecting GW by CMB Polarisation

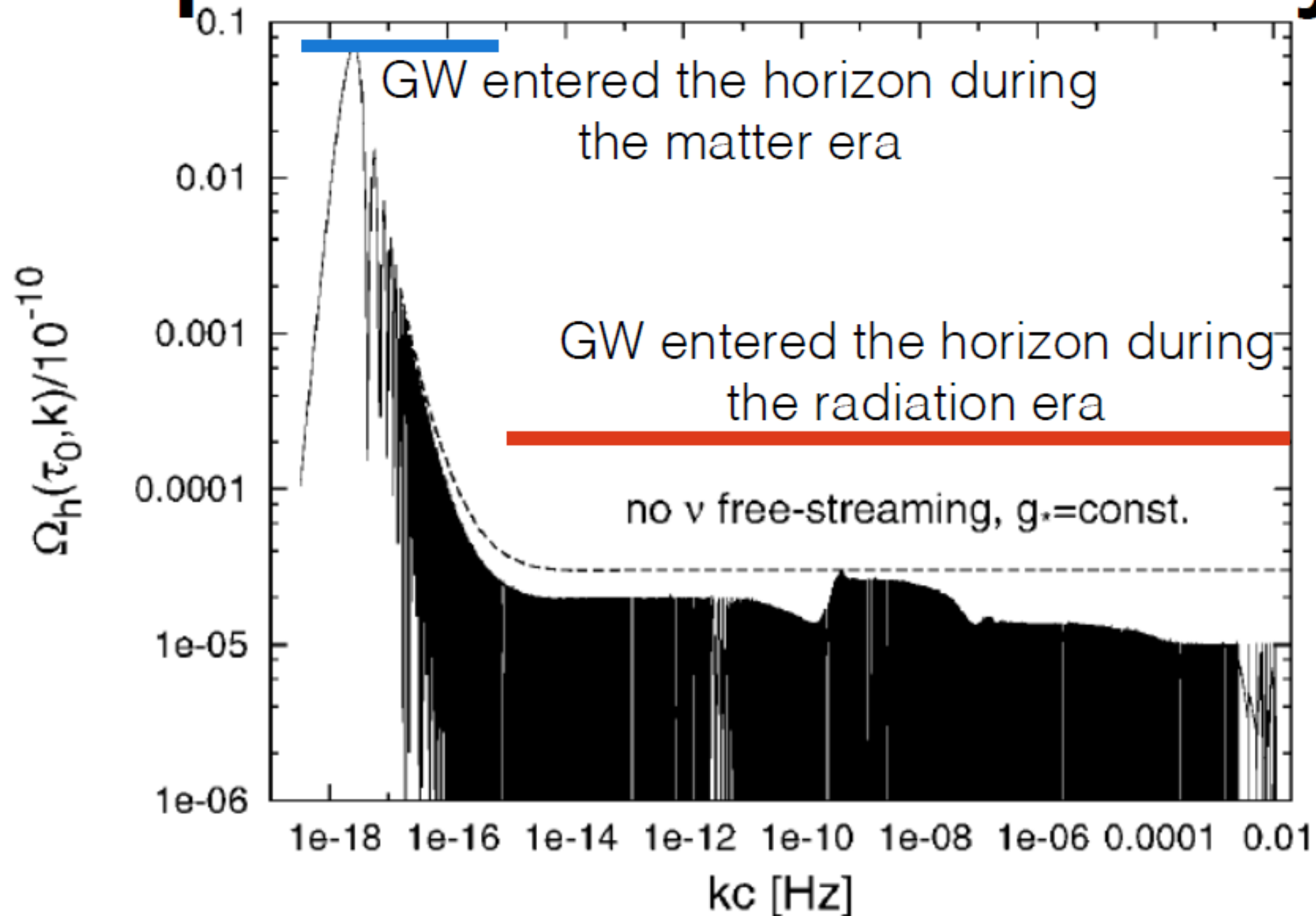


Detecting GW by CMB Polarisation

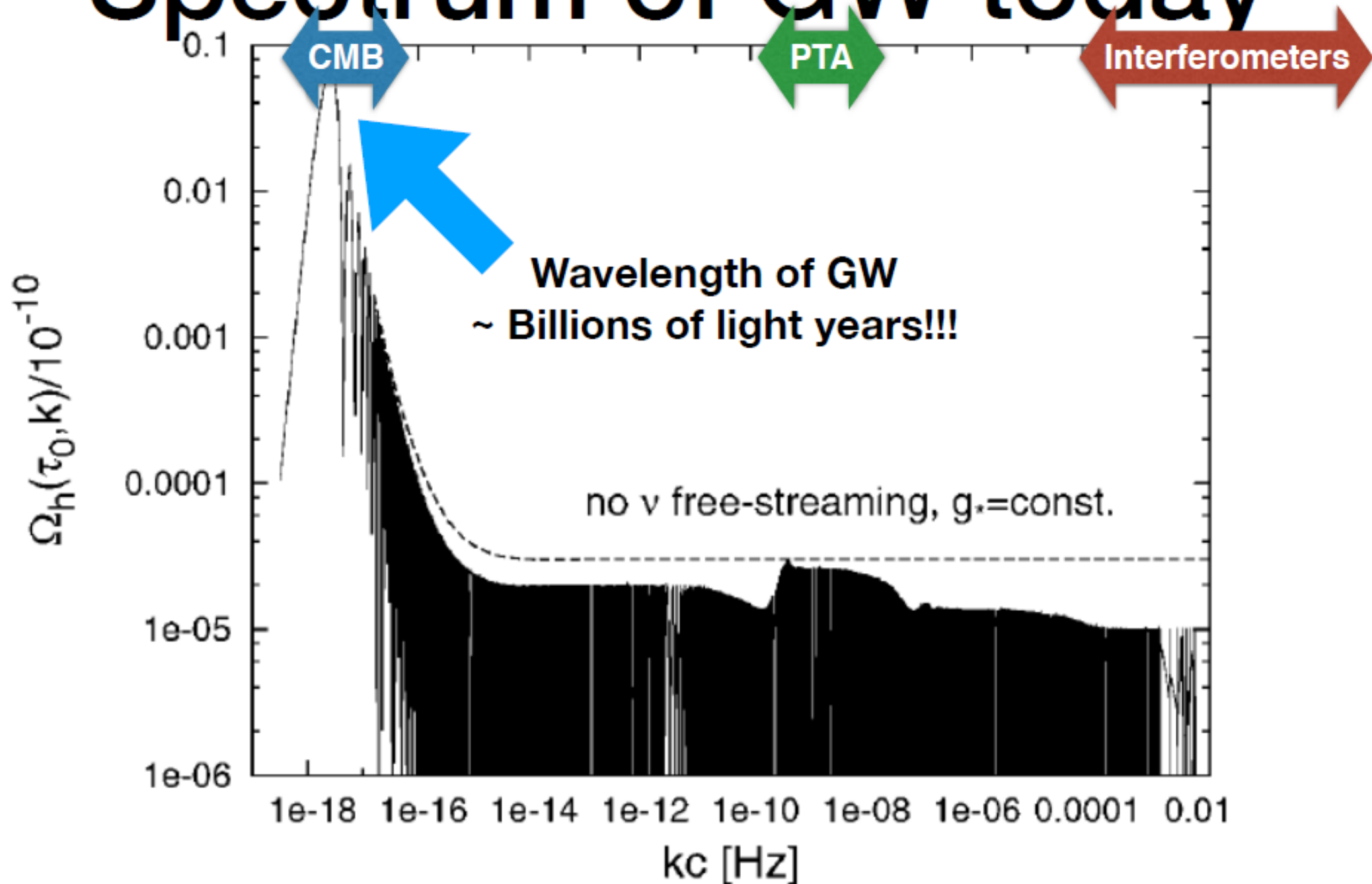
Space is stretched => Wavelength of light is also stretched



Theoretical energy density Spectrum of GW today



Theoretical energy density Spectrum of GW today



Density Field Transfer Function

Early Universe
Primordial Density
Fluctuations



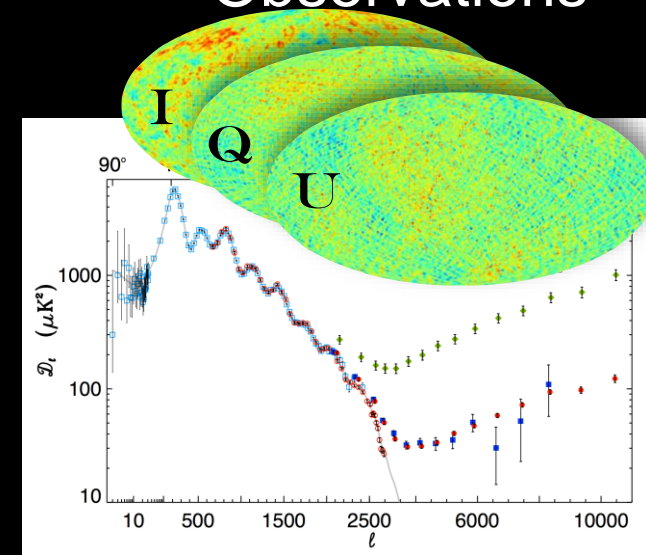
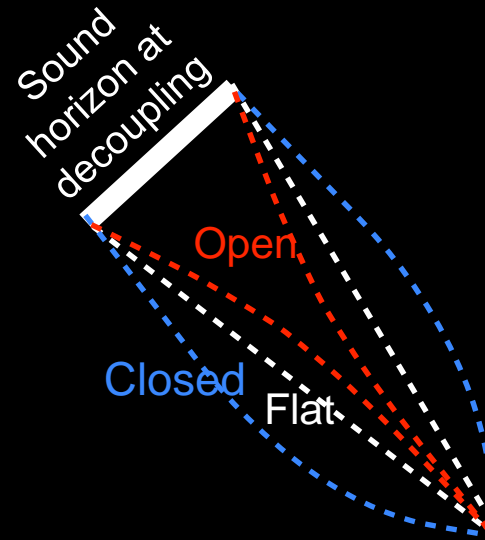
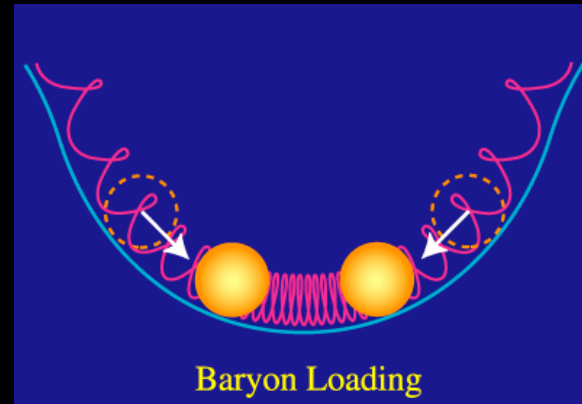
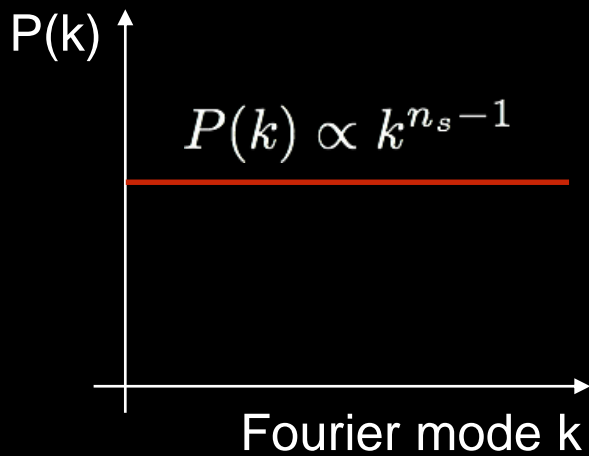
Acoustic
Oscillations



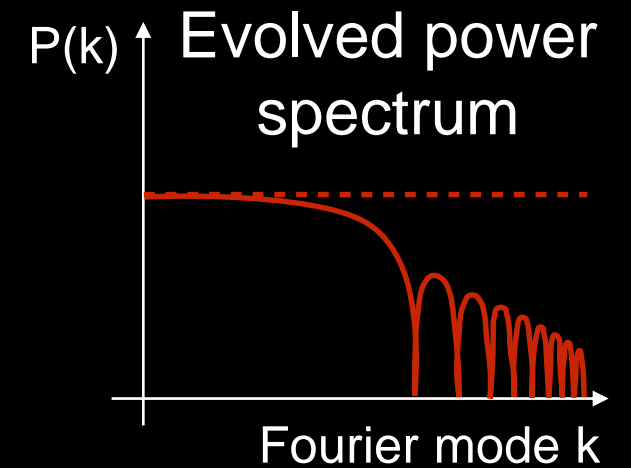
Geometry



CMB
Observations



- Perturbations evolve from end of inflation to decoupling due to matter-radiation oscillations.
- The transfer function depends upon « simple physics » and cosmological parameters
- Allows to fit both cosmology and primordial spectra (including inflationary physics)



Scalar and tensor modes - E & B polarization

- **Scalar perturbations:** $P_s(k) = A_s \left(\frac{k}{k_0} \right)^{n_s - 1}$

- Density fluctuations

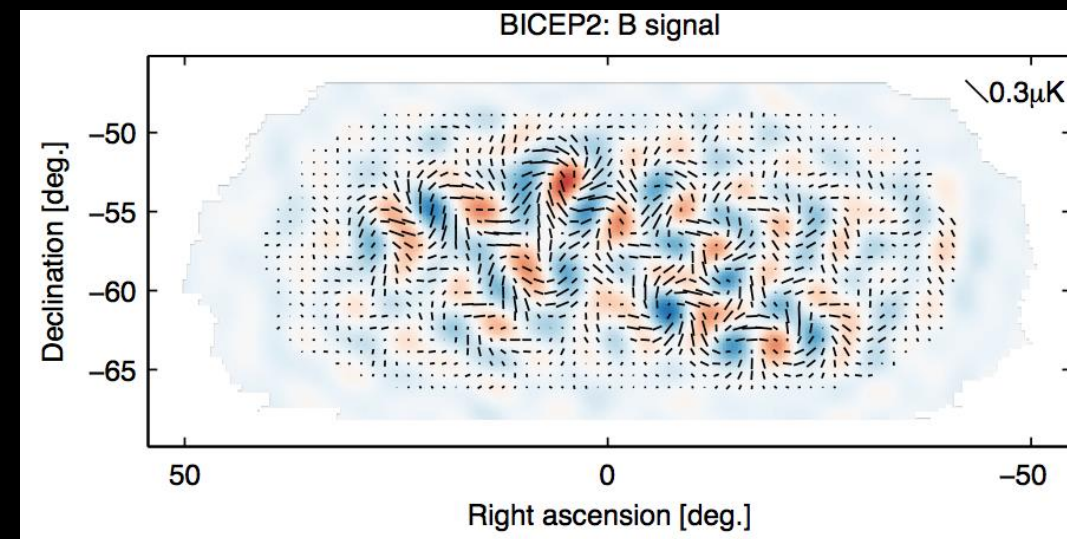
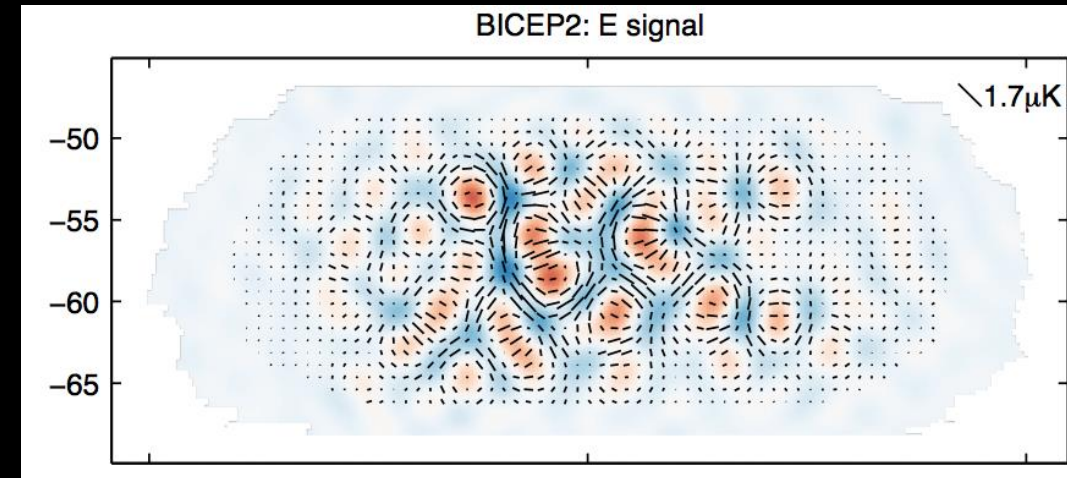
- Temperature
- E polarization
- No B polarization

- **Tensor perturbations:** $P_t(k) = A_t \left(\frac{k}{k_0} \right)^{n_t}$

- Specific prediction from inflation!

- = Primordial gravitational waves

- Temperature
- E polarization
- B Polarization



⇒ detecting primordial B-modes: $r = \frac{P_t(k_0)}{P_s(k_0)}$ ~ ratio between B and E modes

- ▶ Direct detection of tensor modes
- ▶ «smoking gun» for inflation
- ▶ Measurement of its energy scale

$$V^{1/4} = 1.06 \times 10^{16} \text{ GeV} \left(\frac{r_{\text{CMB}}}{0.01} \right)^{1/4}$$



BICEP, Keck

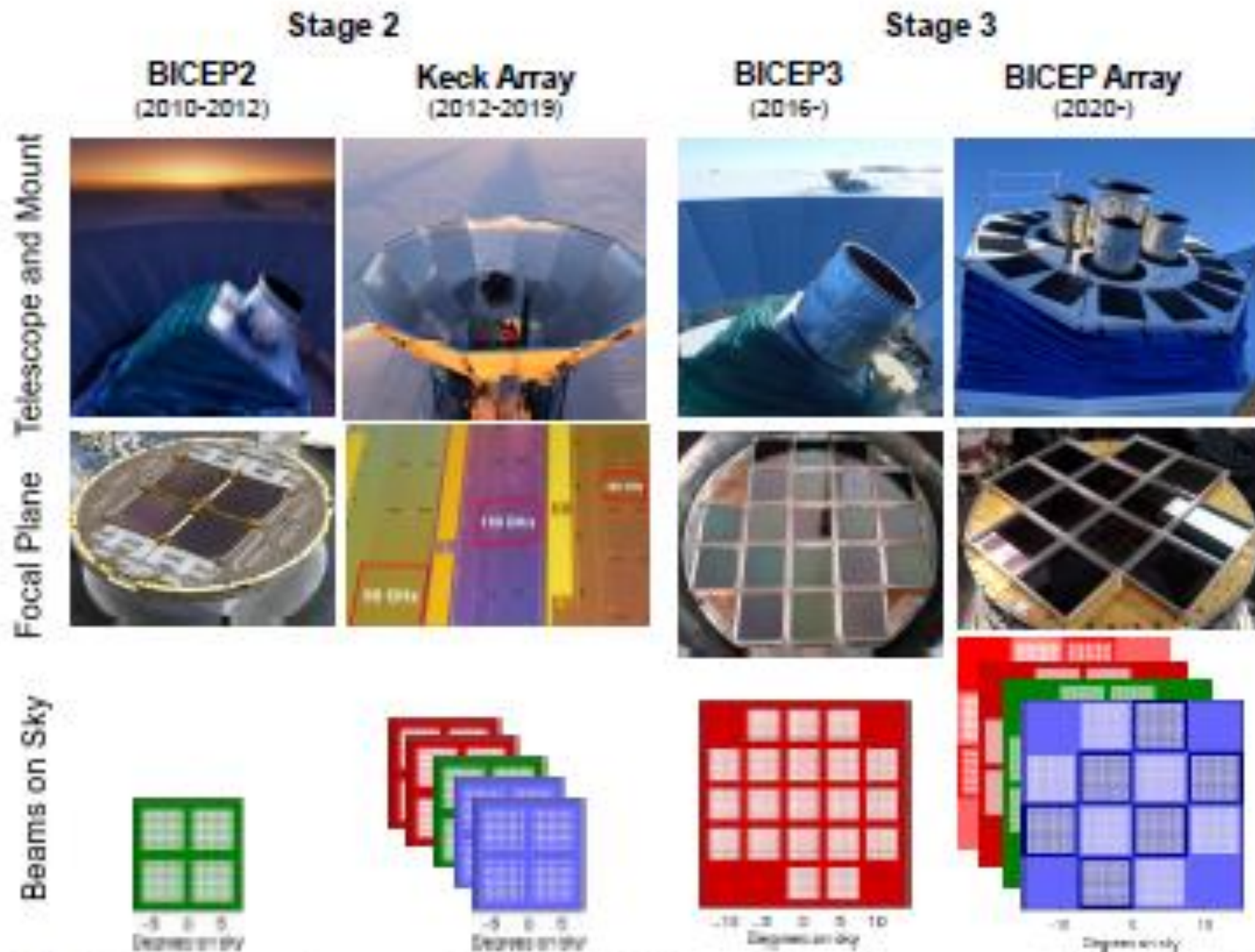


Figure 1. The BICEP/Keck telescopes are Stage-2 and Stage-3 CMB ground-based experiments characterized by $\approx 10^3$ and $\approx 10^4$ detectors respectively. The top two panels show the telescopes (and their physical focal planes) operating since 2010. In the bottom panel, each plane stands for a receiver. The white dots represent the detectors and the beam size as projected on the sky, while the color of a plane denotes the observing frequency. The first receiver (30/40 GHz) of BICEP Array started running in 2020, and it will be fully upgraded to have the other three receivers shown in the figure by 2023.

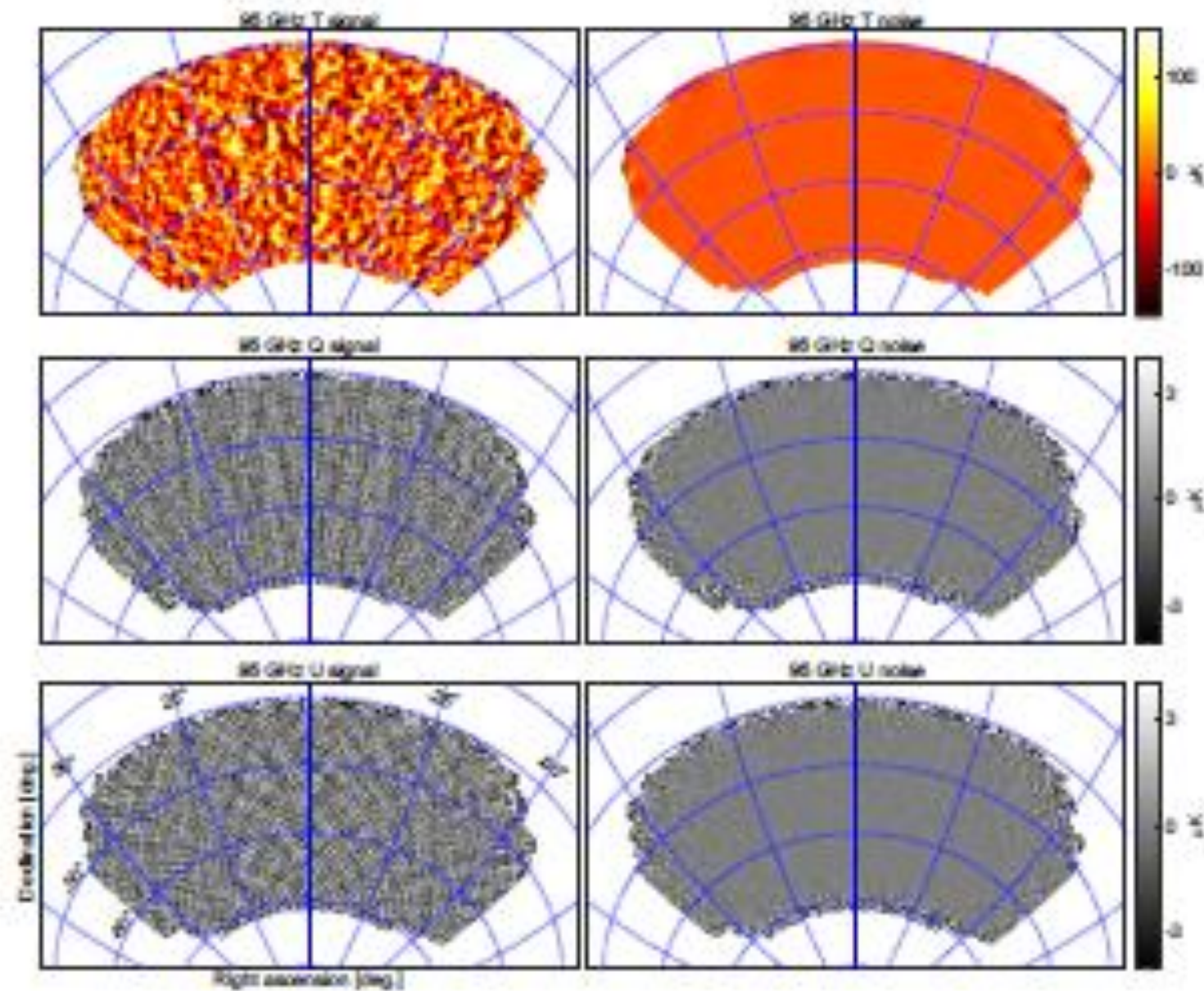
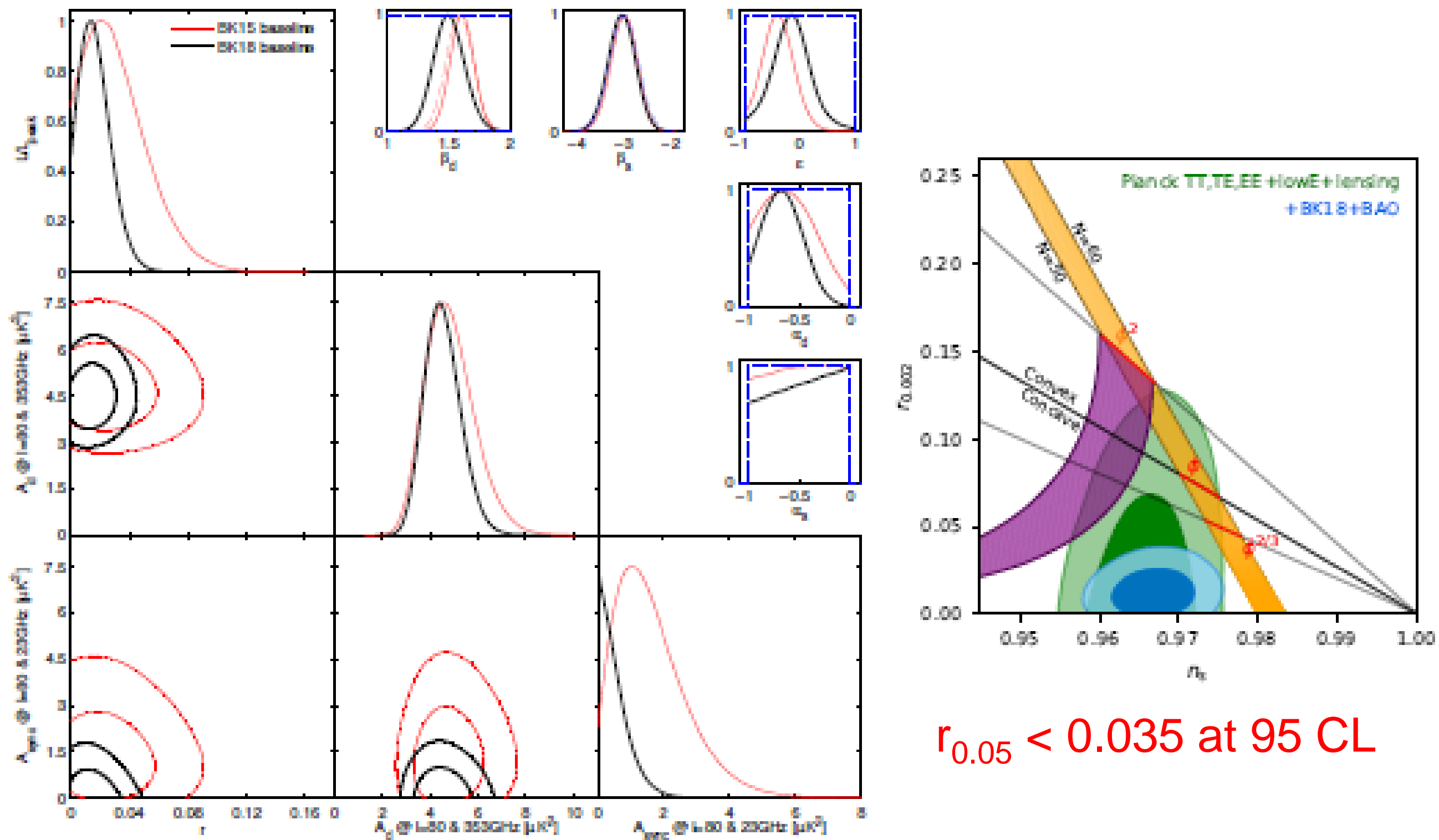


Figure 2. The BICEP3 95 GHz T , Q , U maps from the BK18 paper are displayed in the left column. These signal maps are made using BICEP3 data from the 2016-2018 observing seasons. The right column shows maps of a noise realization produced by randomly and evenly flipping the sign of scan sets during the map coadding process. Note that the signal maps in general appear different from the full-sky measurement of the same sky patch since they are heavily filtered by beam smoothing, timestream processing and deprojection.



$r_{0.05} < 0.035$ at 95 CL

Figure 5. *Left:* CosmoMC likelihood results for the BICEP/Keck baseline model. Selected 1D and 2D marginalized posteriors are shown. The red faint curves are the results from BK15 while the black solid curves are the results of BK18. The dashed blue and red lines show priors on foreground parameters. The analysis method is the same as in BK15, except the β_d prior based on *Planck* data from other regions of the sky is removed this time due to the improved sensitivity of BK18. *Right:* Constraints in the r vs. n_s plane. The purple and orange bands are natural inflation and monomial inflation respectively. The blue contour shows the updated constraint after adding BK18 and BAO data to the *Planck* baseline analysis. The r posterior is tightened from $r_{0.05} < 0.11$ to $r_{0.05} < 0.035$ at 95% confidence.

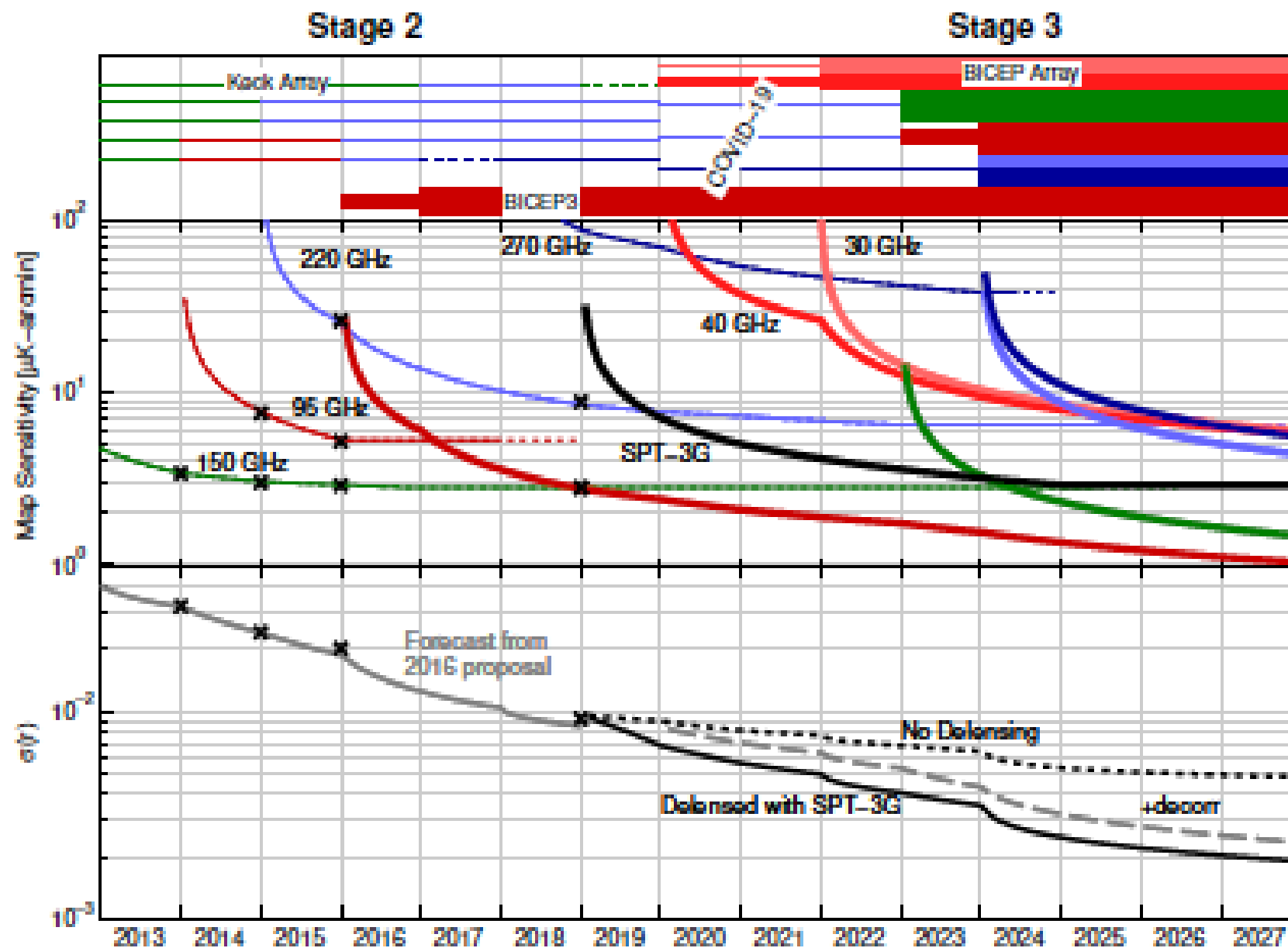
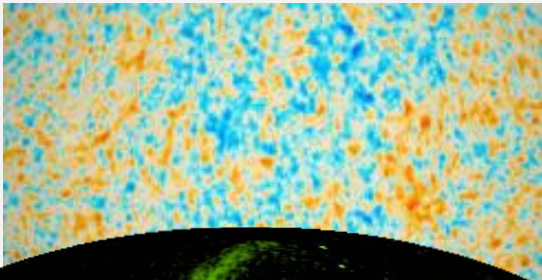


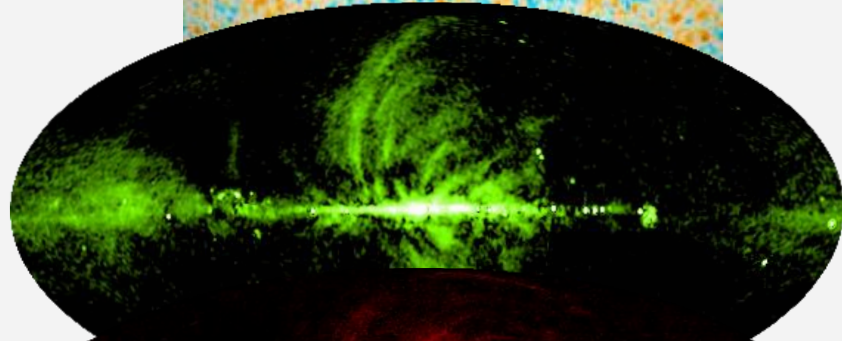
Figure 6. The forecasts for the BICEP/Keck program. The top panel shows the plan of observation. The thickness of each line represents the detector number in a single receiver while its color represents the center frequency labeled in the next panel; the middle panel shows the corresponding map depth over time as lines. The cross marks are published values including those in BK15 and BK18. The sensitivity beyond 2018 is predicted by scaling based on achieved performance. The black SPT-3G line is the combined 95/150 GHz map depth projected from the achieved sensitivity in the 2019 and 2020 seasons; the bottom panel transforms map depth into $\sigma(r)$. Cross marks are again the published values. The good agreement between these cross marks and projection lines indicates that the forecasting method is realistic. Two independent forecasts (solid and dotted lines) highlight the significance of delensing. Including dust decorrelation in the delensing case (the dashed line) results in slightly higher $\sigma(r)$.

BICEP/Keck collaboration arXiv:2203.16556
M. Tristram et al Phys Rev D 105, 083524 (2022)
P. Campet, E. Komatsu arXiv:2205.05617

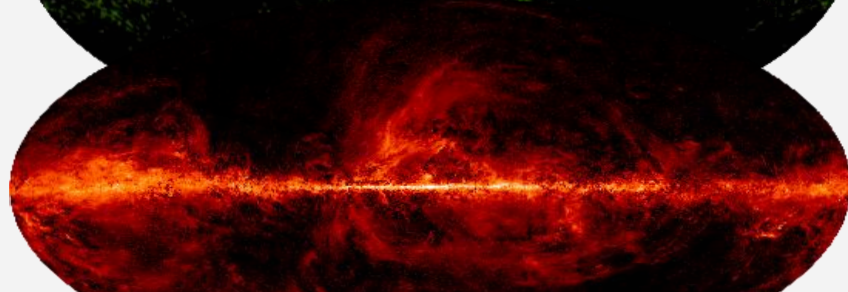
Problematic of foregrounds



CMB



Synchrotron



Dust

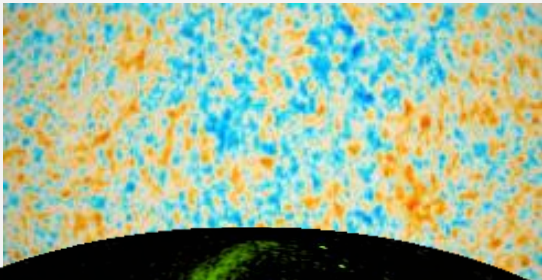


Atmosphere

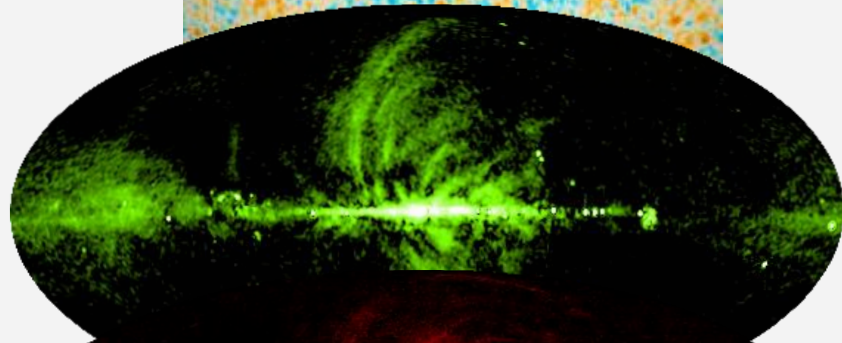


Sum of several emissions

Problematic of foregrounds



CMB



Synchrotron



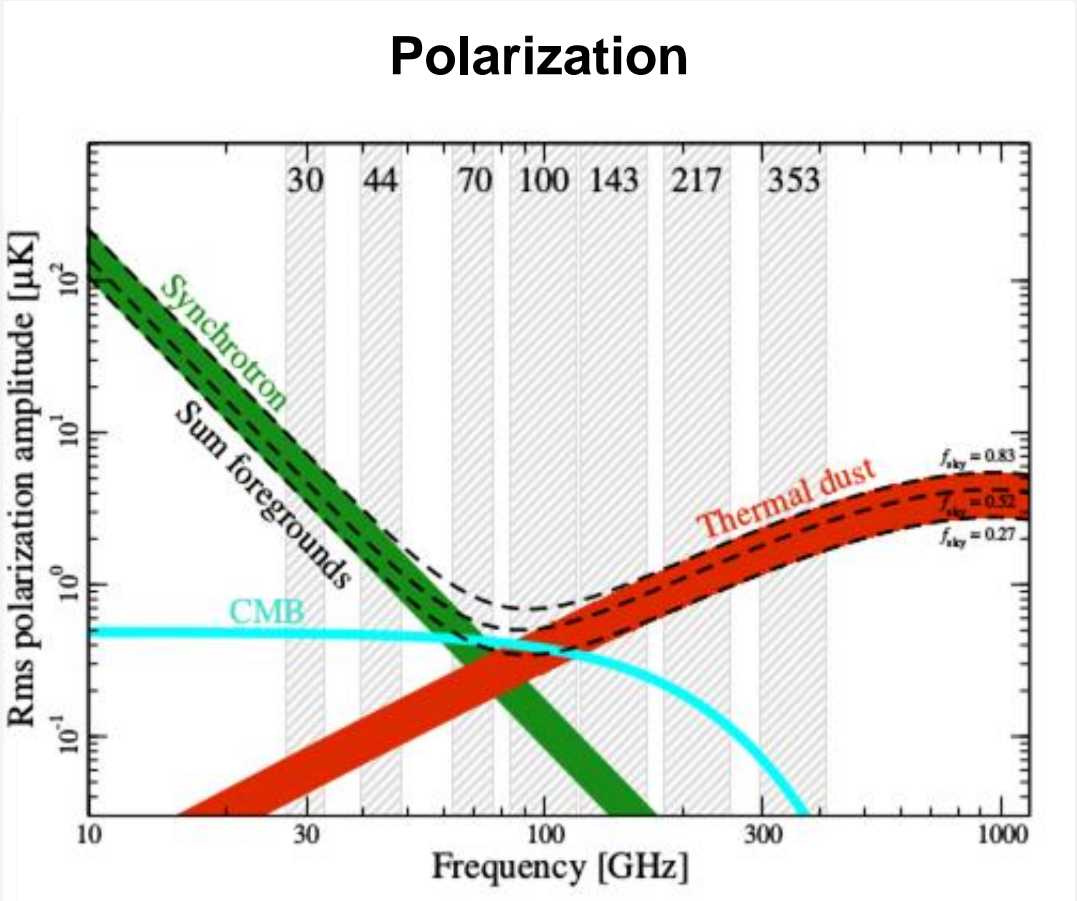
Dust



Atmosphere

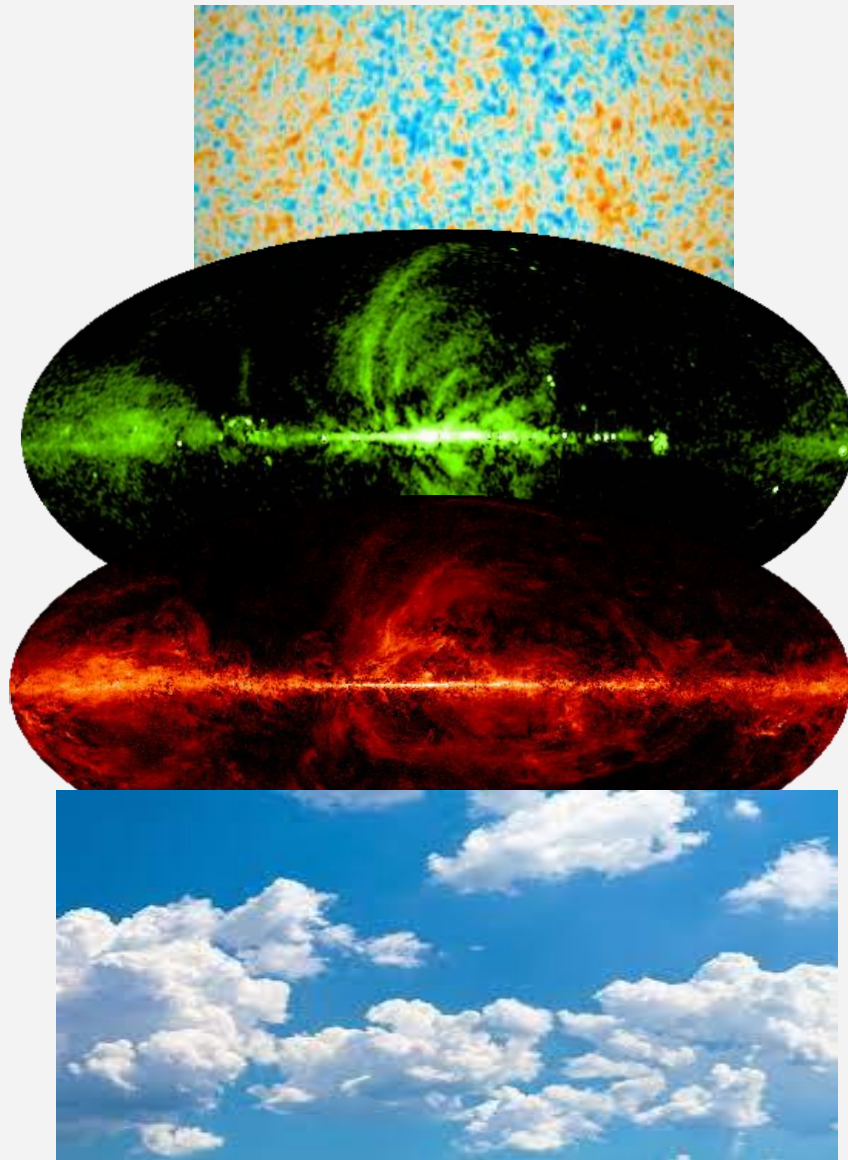


Sum of several emissions



Credit : Planck

Problematic of foregrounds



CMB

Synchrotron

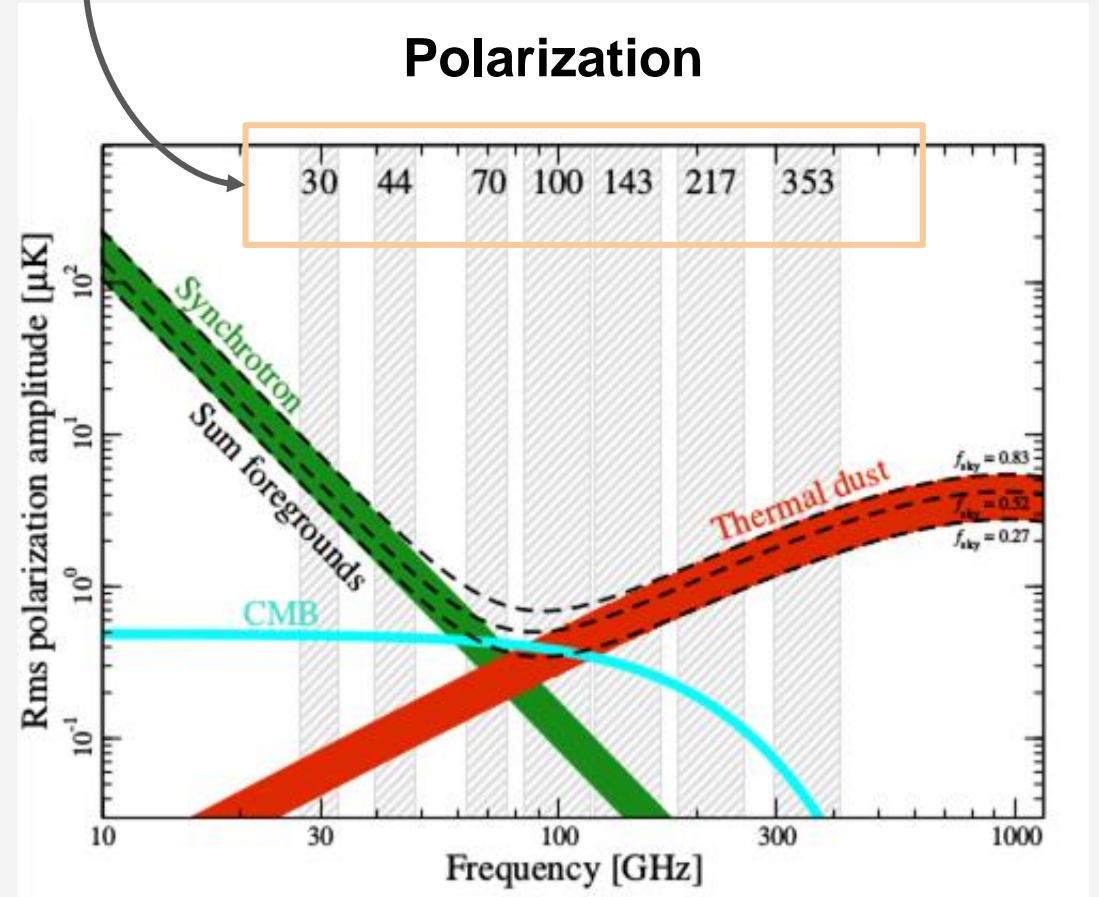
Dust

Atmosphere



Sum of several emissions

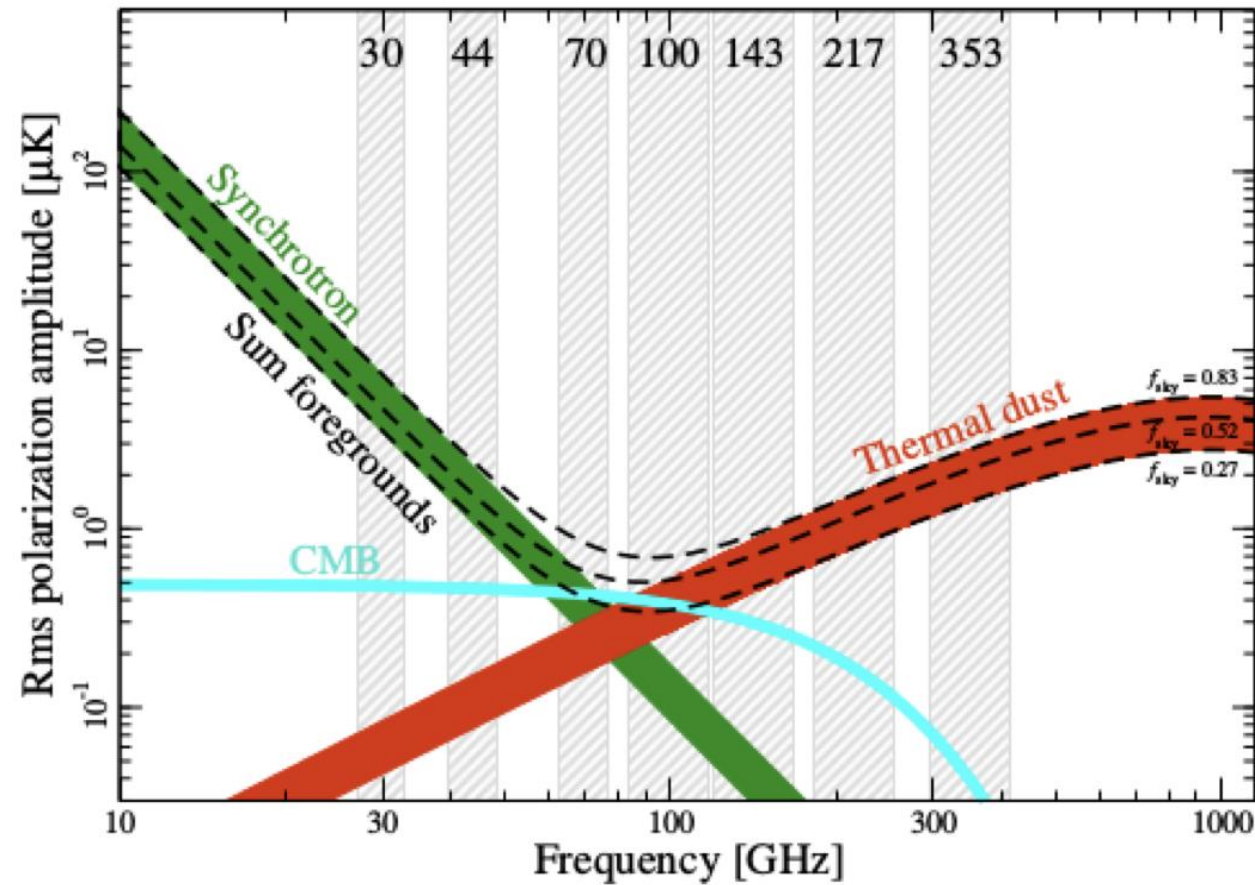
Observation at distinct frequencies is needed



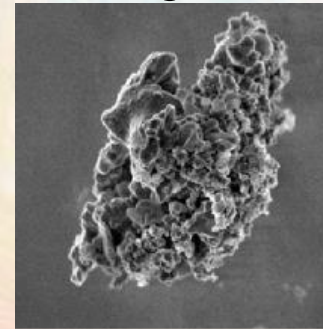
Credit : Planck

Galactic Foregrounds

Polarization

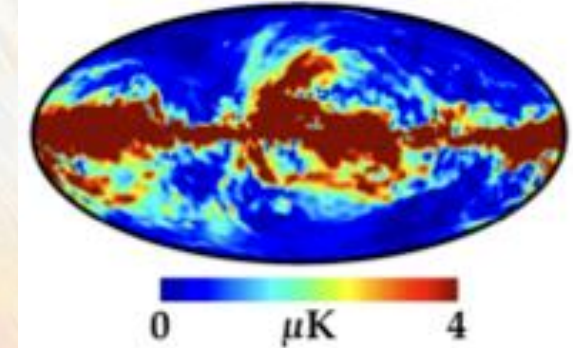


Dust grains

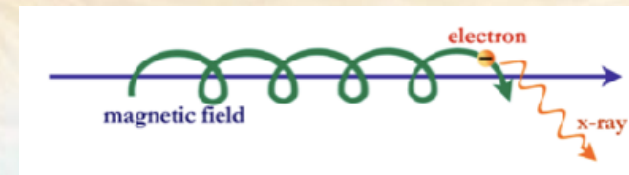


Thermal dust

From Planck-353 rescaled @100GHz

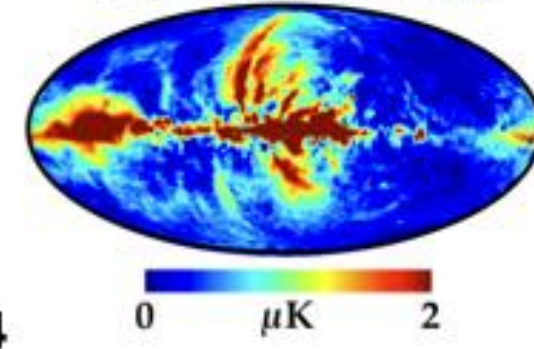


Synchrotron



Synchrotron

From WMAP-K rescaled @100GHz

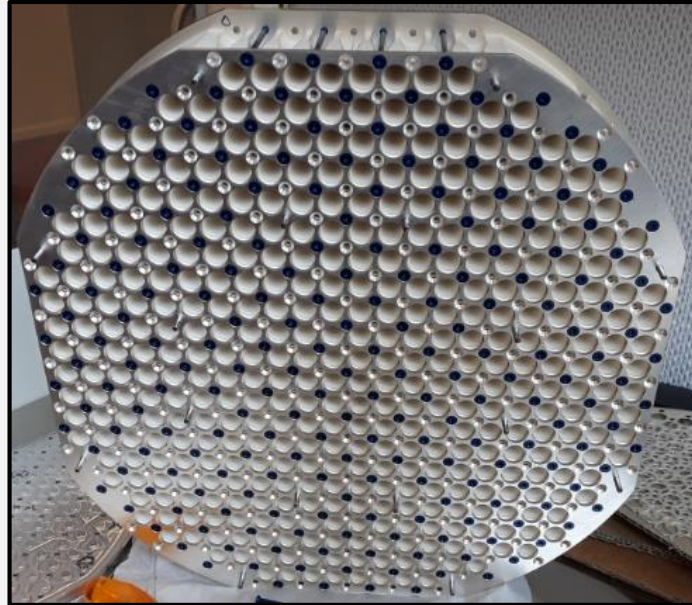


[N. Krachmalnicoff]

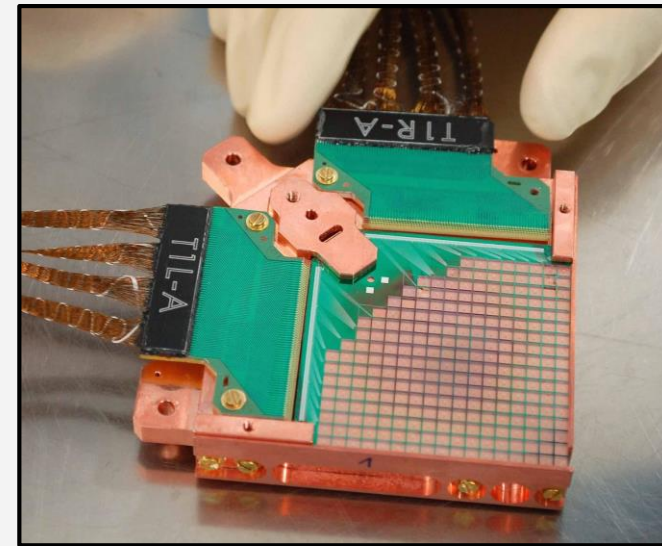
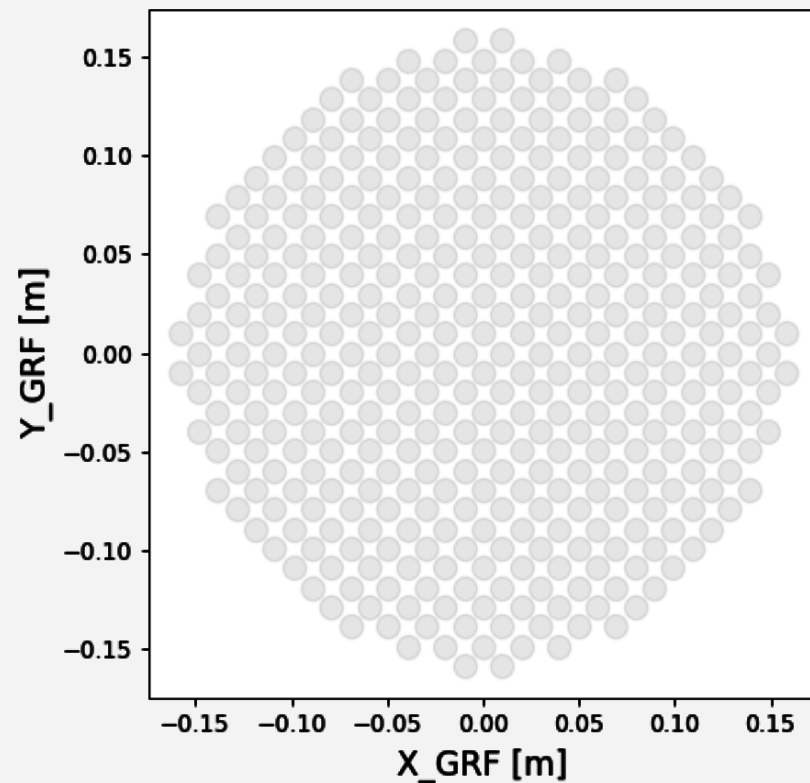
Many efficient foreground cleaning techniques exist. They rely on multiwavelength observations. But they usually assume “smoothness” of the foreground EM spectrum...

[Back to Index](#)

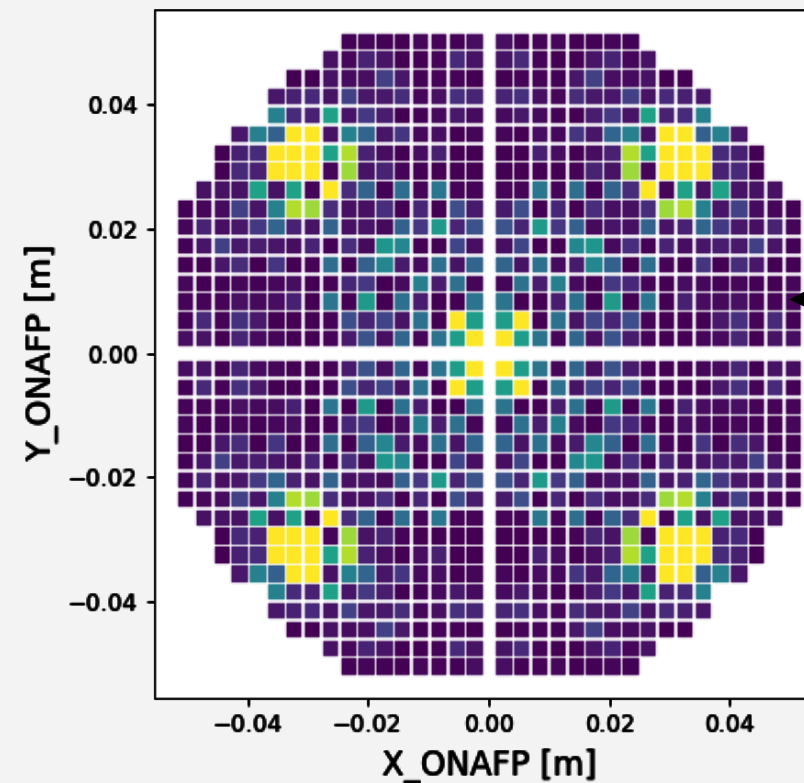
QUBIC, the bolometric interferometer



Horn array



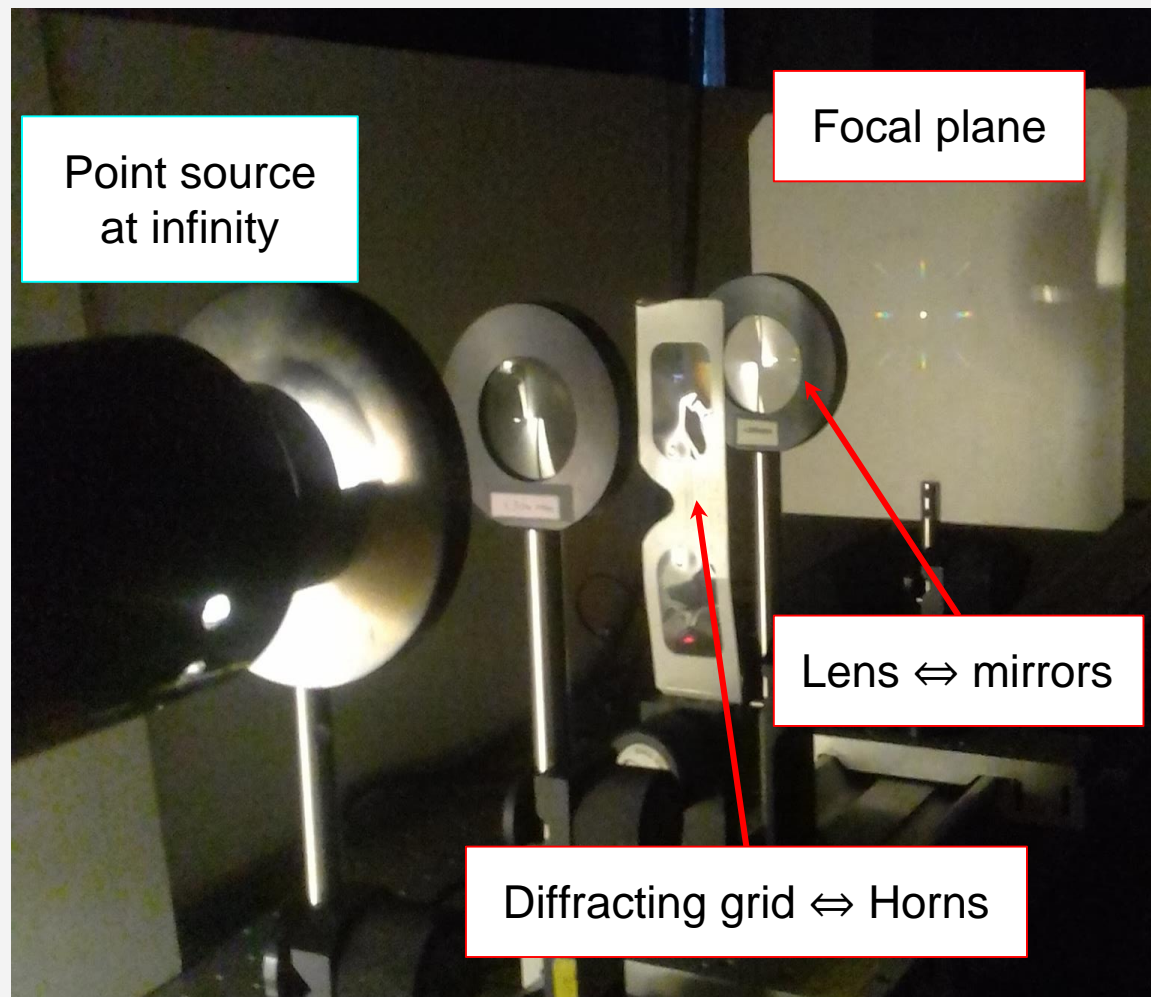
Focal plane : bolometers (TES)



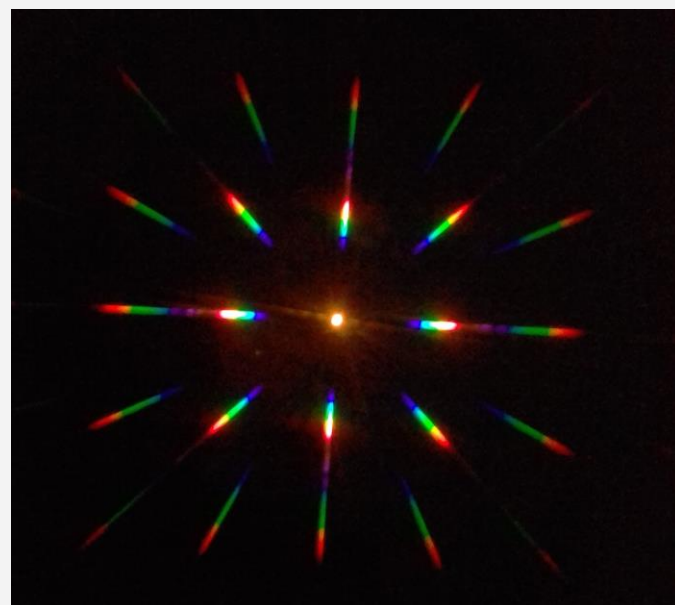
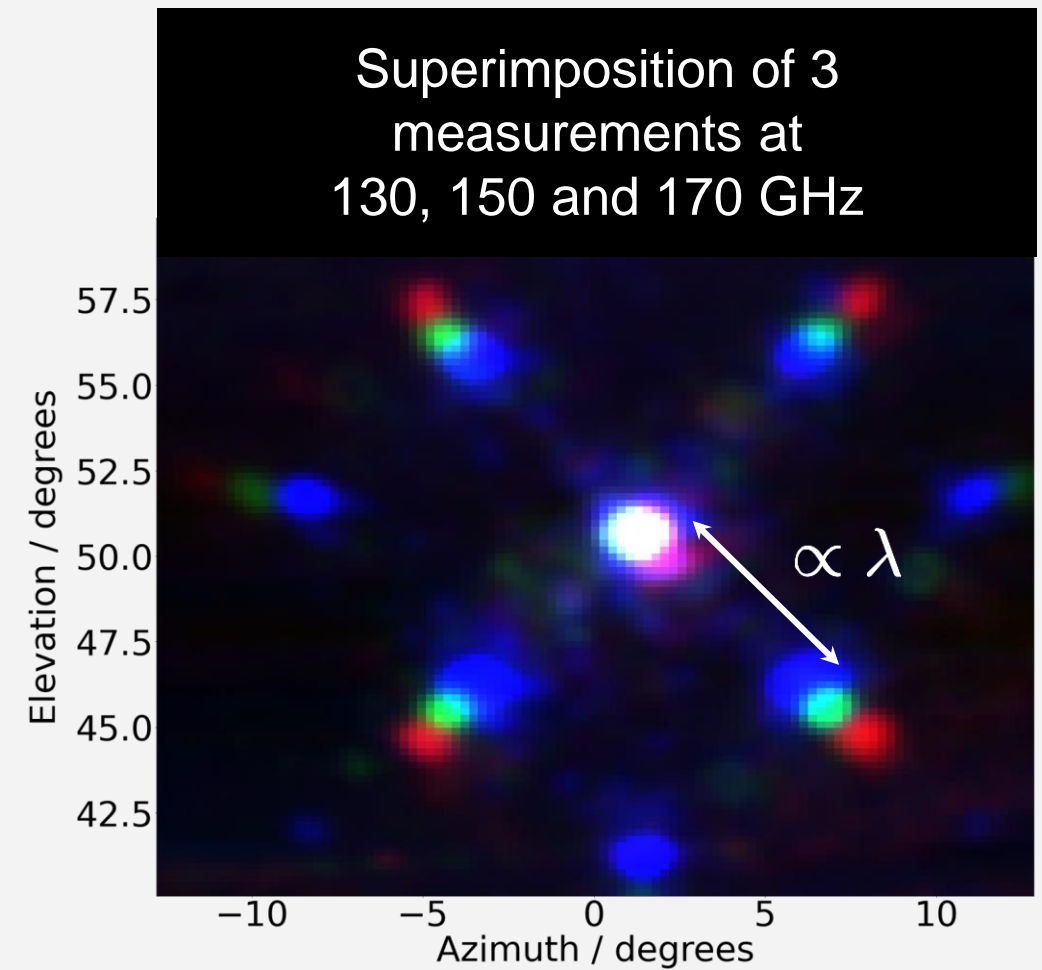
PSF : Response of the instrument on the focal plane for one direction on the sky, at one wavelength.

Spectral imaging

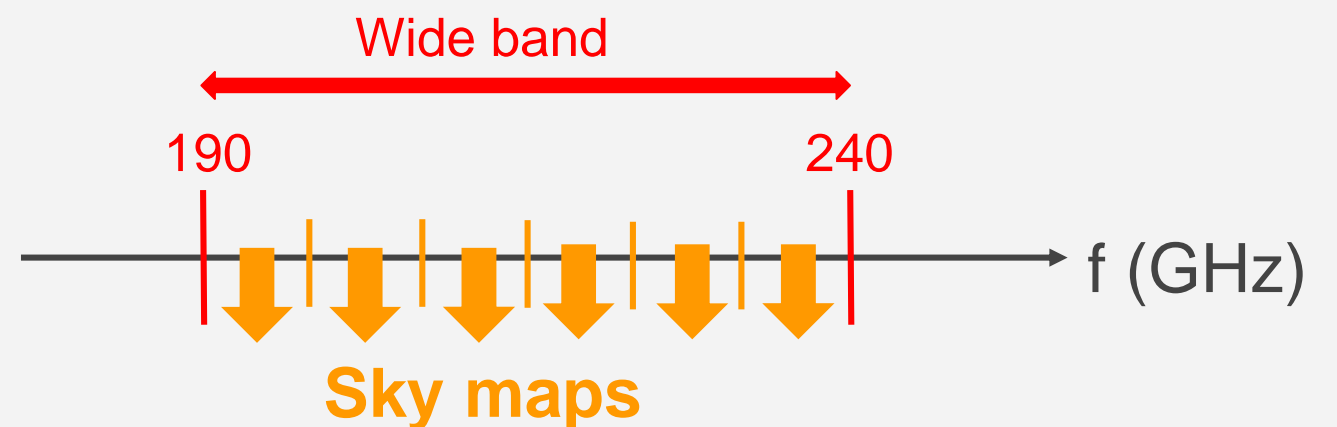
[Mousset, Gamboa et al, QUBIC II, JCAP]



Spectrale information is spatially encoded

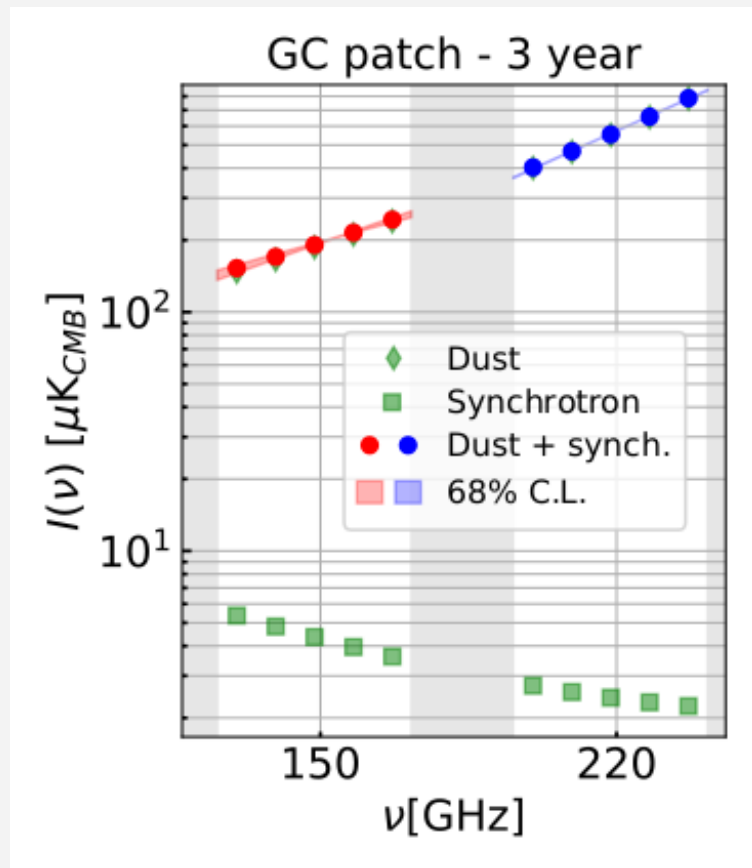


Bolometers **integrate the signal** in a wide frequency band. Spectral imaging allows to split the band in **sub-bands** during the **post-processing**.

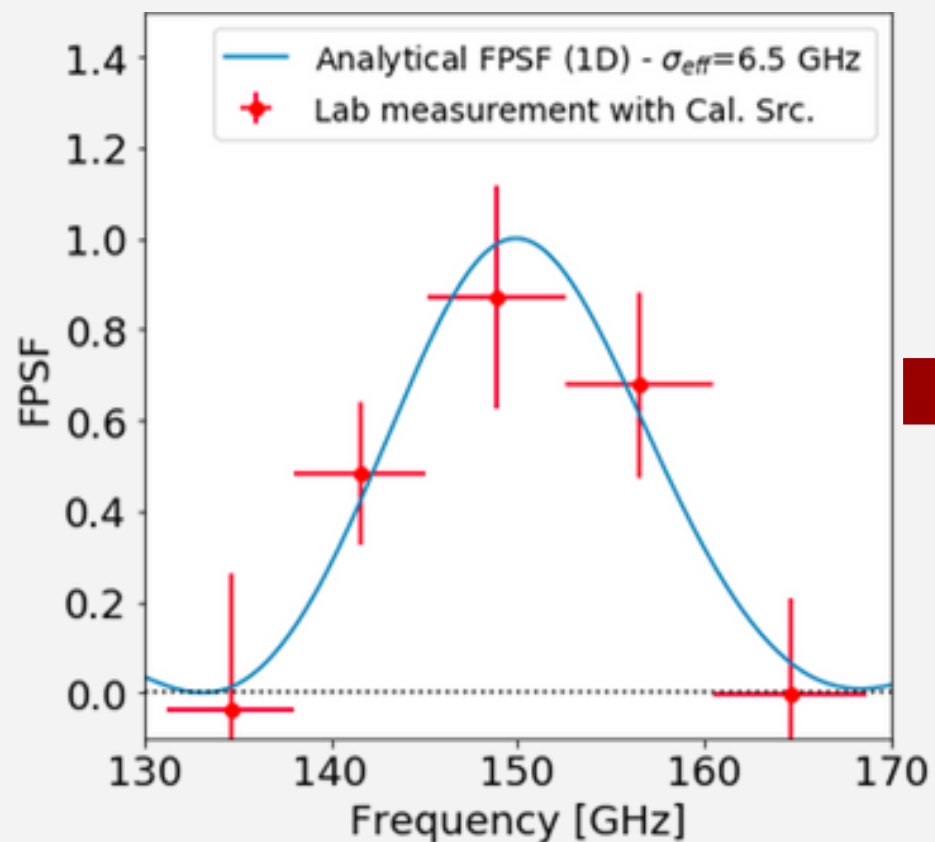


A potential lever arm to control foregrounds

Work in progress



Constrain complex Spectral Energy Density (SED) models



Detect monochromatic emissions (for example CO lines)

Installation in Argentina



Observation of the sky from Salta in October



Re-assembling in Salta

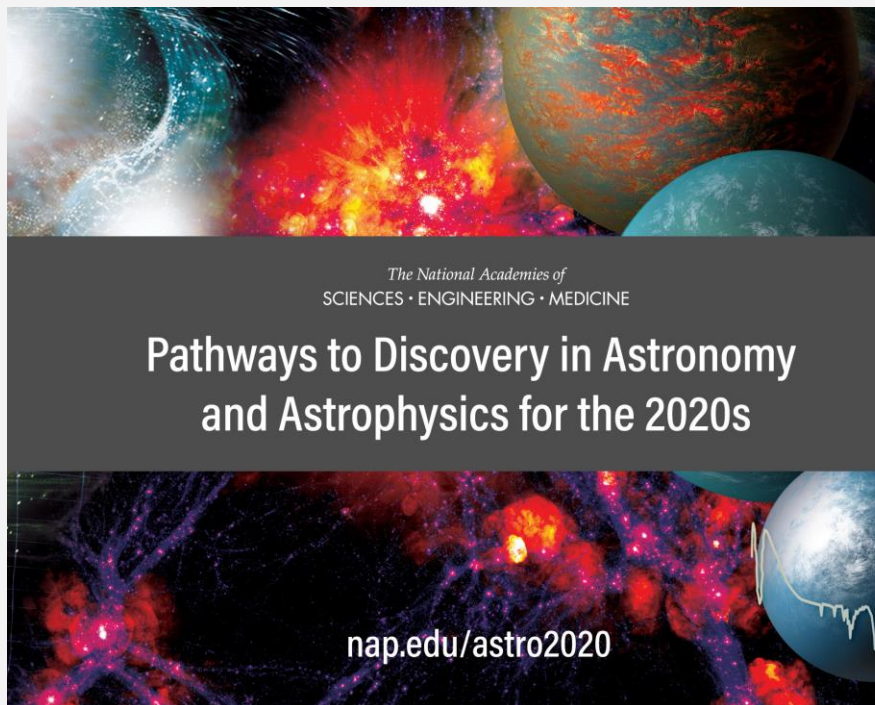


**Observation site:
San Antonio de Los Cobres, ~5000 m**

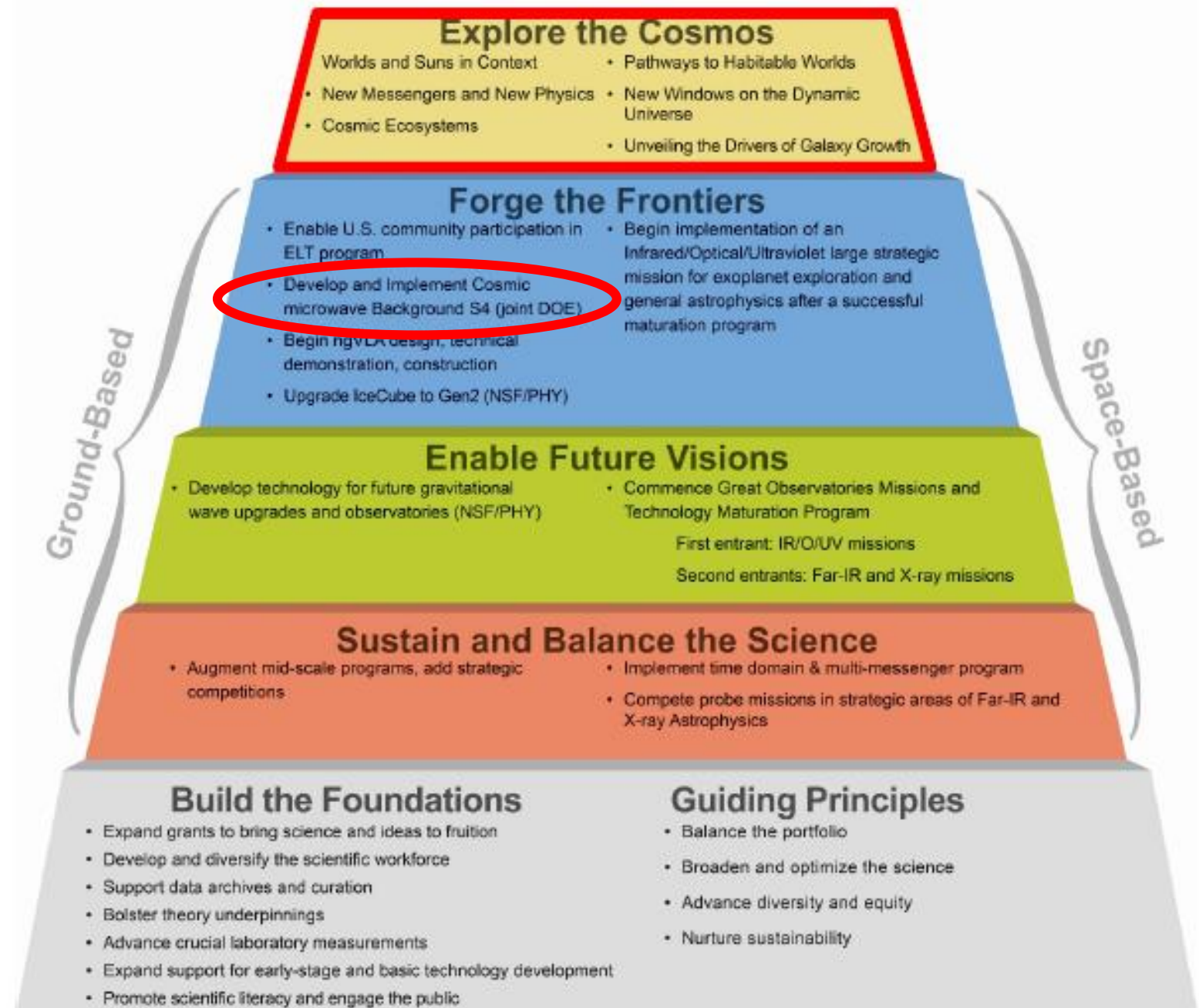


US Decadal Survey

nap.edu/astro2020



Realizing the Astro2020 Program: Pathways From Foundations to Frontiers



The Cosmic Microwave Background Stage 4 Observatory



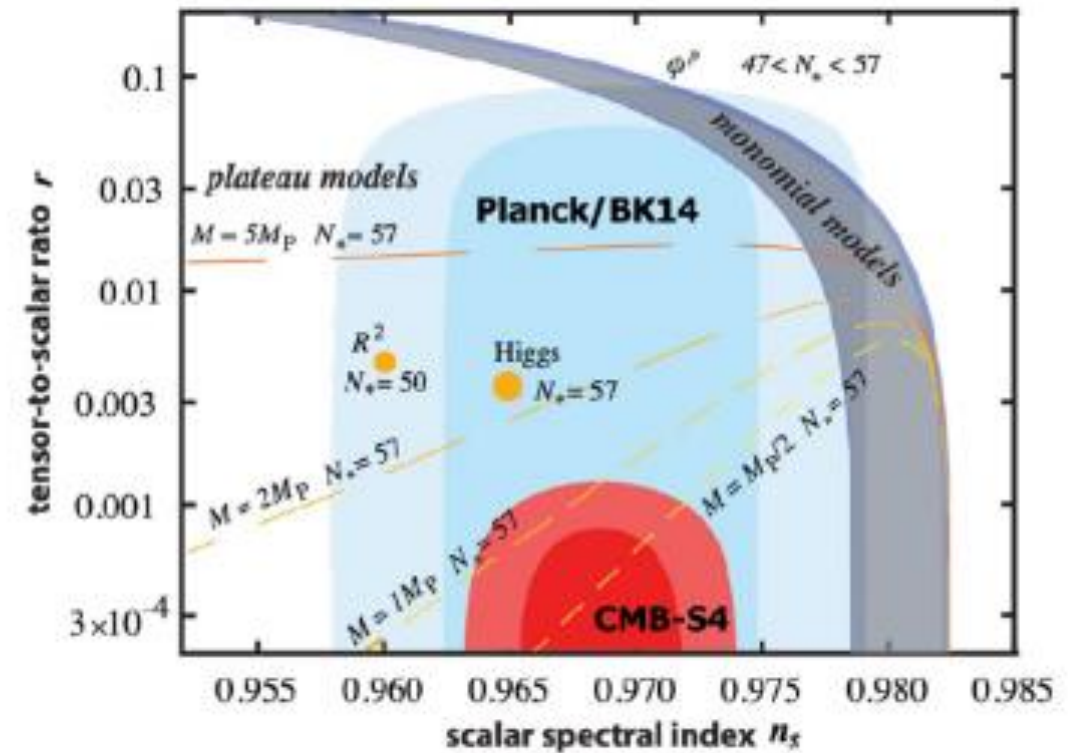
CMB-S4 builds on the foundation of decades of CMB measurements to take a major leap, pushing CMB science to the next level

Scientific goals

B-mode CMB polarization signatures of primordial gravitational waves and inflation

Maps 50% sky, every other day from 0.1- 1 cm with unprecedented sensitivity

Broad science including systematic time domain science



CMB-S4 consists of a systematically planned suite of facilities in Antarctica and Chile designed to sample a wide range of independent frequencies, and probe a combination of large and small angular scales

CERN COURIER

March/April 2022 cerncourier.com

Reporting on international high-energy physics

CMB-S4 SETS SIGHTS ON THE EARLY UNIVERSE

APPEC town meeting Berlin
2022

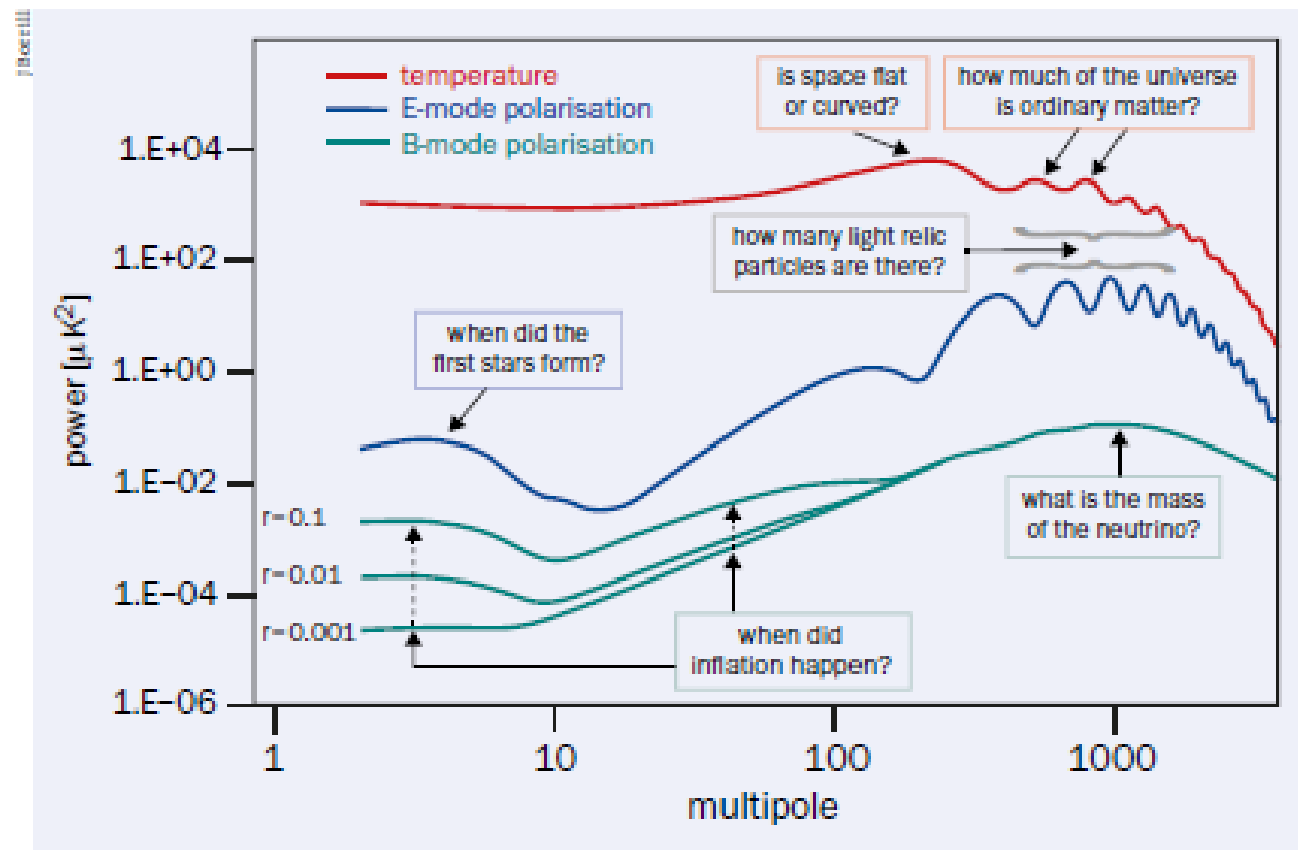
Countdown to LHC Run 3

Leptons beyond the Standard Model

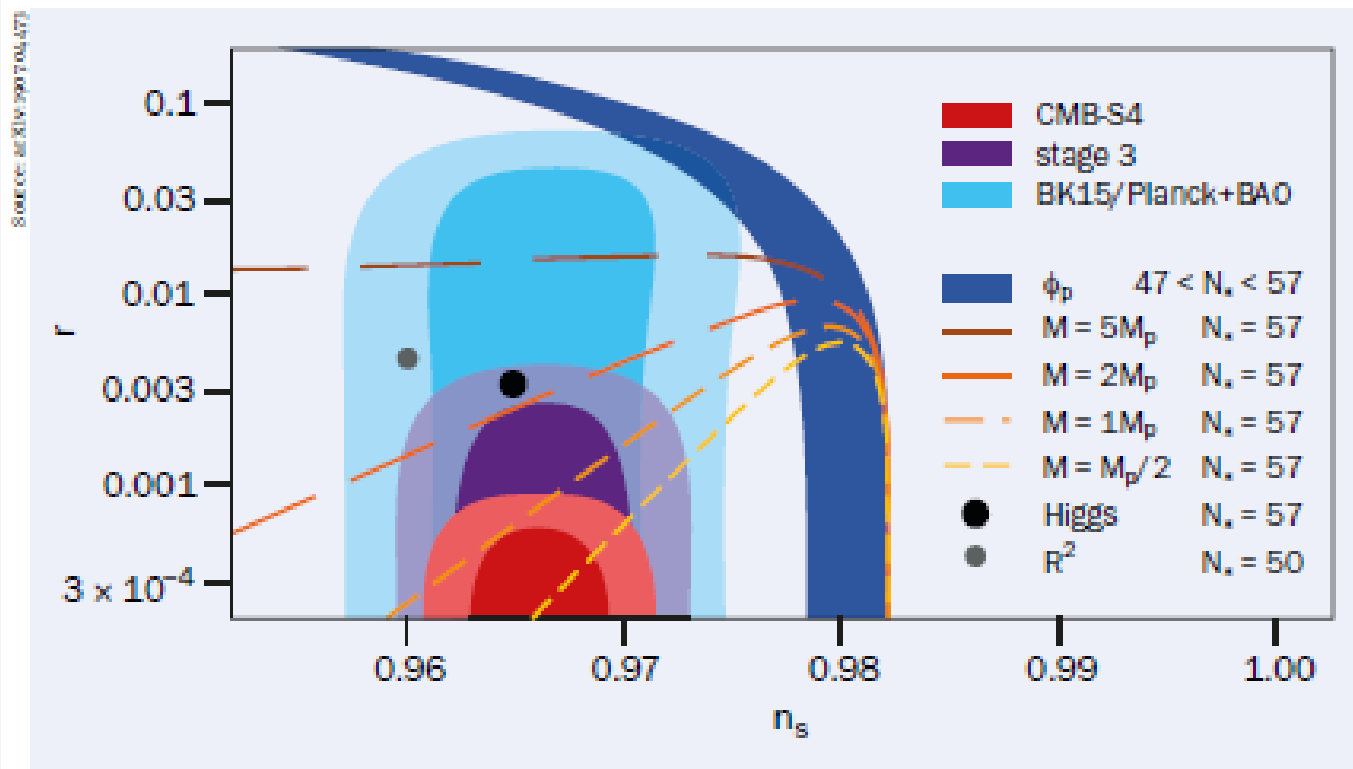
Sustainable development

On the cover: *CMB-S4 constraints on inflation, flipped for presentation purposes. 36*

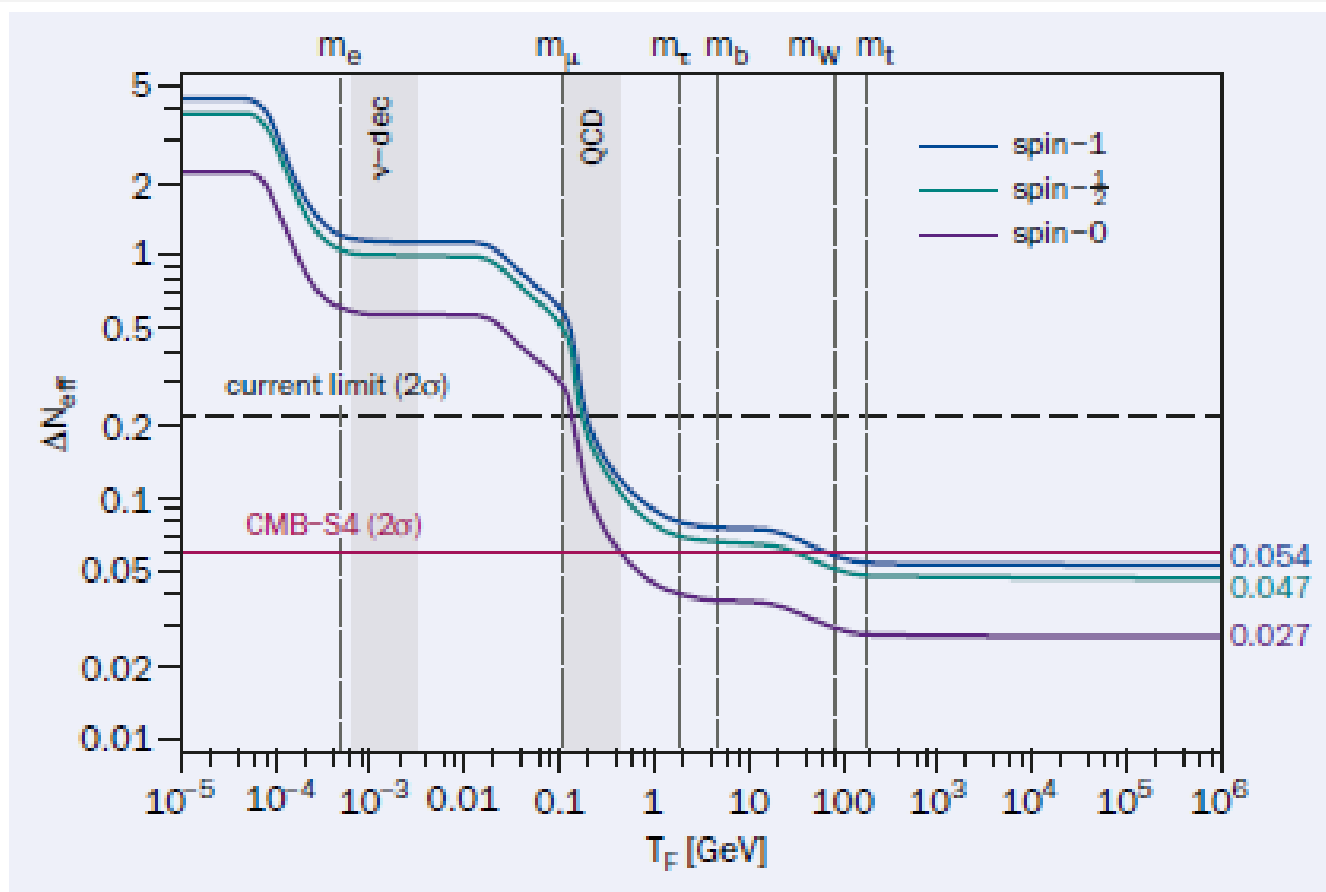




Power spectra The temperature and polarisation power spectra of the CMB, illustrating features that can answer key questions in cosmology and fundamental physics. The CMB polarisation is decomposed into a curl-free E-mode and divergence-free B-mode by analogy with electromagnetism, with r quantifying the scalar-to-tensor ratio (the size of the B-modes relative to that of the temperature power spectrum).



Constraining inflation Current (light blue and purple) and anticipated (red) CMB-S4 constraints on the scalar-to-tensor ratio r compared with the predictions of various inflationary models that naturally explain the observed value of the spectral “tilt” of the power spectrum, $n_s = 0.965$. The popular Starobinsky and Higgs inflation models are shown as grey and black circles. The lines show models with different masses of the inflaton in units of the Planck mass M_p and N_* is the number of e -folds. The corresponding inflation potentials ϕ_p all either polynomially or exponentially approach a plateau.



Source: arXiv:0907.0497

Light relics Current (black) and anticipated (magenta) CMB-S4 constraints on the effective number of light-relic species $N_{\text{eff}} = N_{\text{SMeff}} + \Delta N_{\text{eff}}$, with $N_{\text{SMeff}} = 3.045$ from neutrinos. The plot shows the contributions of a single massless particle (which decoupled from the SM at freeze-out temperature T_F) to N_{eff} , with the displayed values on the right indicating observational thresholds for particles with different spins.



Looking up The full facility will employ 18 0.5 m small-aperture telescopes (top left), three per mount, fielding 150,000 detectors; one 5 m large-aperture telescope (right) fielding 130,000 detectors; and two 6 m large-aperture telescopes fielding 275,000 detectors (bottom left).

CMB-S4